Developmental Biology 453 (2019) 155–167

Contents lists available at ScienceDirect

Developmental Biology

journal homepage: www.elsevier.com/locate/developmentalbiology

Transcriptional profiling of murine retinas undergoing semi-synchronous cone photoreceptor differentiation

Michael L. Kaufman [a], Ko Uoon Park [a], Noah B. Goodson [a], Shereen Chew [c], Stephanie Bersie [a], Kenneth L. Jones [b], Deepak A. Lamba [c], Joseph A. Brzezinski IV [a,*]

[a] Department of Ophthalmology, University of Colorado Anschutz Medical Campus, Aurora, CO, USA
[b] Department of Pediatrics, University of Colorado Anschutz Medical Campus, Aurora, CO, USA
[c] Eli and Edythe Broad Center of Regeneration Medicine and Stem Cell Research, Department of Ophthalmology, University of California, San Francisco, CA, USA

ARTICLE INFO

Keywords:
Cone photoreceptor
γ-secretase inhibition
Retinal development
Fate specification
RNA-Seq
Retinal organoid

ABSTRACT

Uncovering the gene regulatory networks that control cone photoreceptor formation has been hindered because cones only make up a few percent of the retina and form asynchronously during development. To overcome these limitations, we used a γ-secretase inhibitor, DAPT, to disrupt Notch signaling and force proliferating retinal progenitor cells to rapidly adopt neuronal identity. We treated mouse retinal explants at the peak of cone genesis with DAPT and examined tissues at several time-points by histology and bulk RNA-sequencing. We found that this treatment caused supernumerary cone formation in an overwhelmingly synchronized fashion. This analysis revealed several categorical patterns of gene expression changes over time relative to DMSO treated control explants. These were placed in the temporal context of the activation of *Otx2*, a transcription factor that is expressed at the onset of photoreceptor development and that is required for both rod and cone formation. One group of interest had genes, such as *Mybl1*, *Ascl1*, *Neurog2*, and *Olig2*, that became upregulated by DAPT treatment before *Otx2*. Two other groups showed upregulated gene expression shortly after *Otx2*, either transiently or permanently. This included genes such as *Mybl1*, *Meis2*, and *Podxl*. Our data provide a developmental timeline of the gene expression events that underlie the initial steps of cone genesis and maturation. Applying this strategy to human retinal organoid cultures was also sufficient to induce a massive increase in cone genesis. Taken together, our results provide a temporal framework that can be used to elucidate the gene regulatory logic controlling cone photoreceptor development.

1. Introduction

The vertebrate retina is an extension of the central nervous system that detects, processes, and relays visual information to the brain. The neural retina is a complex multi-layered tissue that harbors seven major cell types, six neuronal and one glial. Within the outer nuclear layer (ONL) reside the two primary light sensing cells: rod and cone photoreceptors. Rods are responsible for sight in low light conditions, while cones are required for color and high acuity daytime vision. Some of the most debilitating visual impairment in humans results from the loss or dysfunction of cone photoreceptors. Cones and the other six major cell types within the neural retina are derived from a pool of retinal progenitor cells (Cepko, 2014). Progenitors permanently exit the cell cycle ("birthdate") and give rise to each retinal cell type in a stereotypical, yet overlapping fashion (Carter-Dawson and LaVail, 1979; la Vail et al., 1991; Rapaport and Vietri, 1991; Wong and Rapaport, 2009; Young, 1985). These cells become specified to a particular fate and then acquire their mature morphology, connectivity, and function. Cone photoreceptors form relatively early in both human and rodent development. In mice, cones permanently exit the cell cycle from embryonic (E) day 12 to E19, with their peak genesis occurring around E14.5 (Carter-Dawson and LaVail, 1979). This peak overlaps with the genesis of other retinal neurons, primarily horizontal, amacrine, and ganglion cells. In rodents and humans, rods massively outnumber cones, such that cones represent just a few percent of the total cells in the retina (Jeon et al., 1998; Sloan et al., 1990). Their rarity and their birthdating overlap with other retinal cell types has made it difficult to uncover the gene regulatory events that control cone photoreceptor genesis.

Transcription factors control fate specification events during retinal development. The homeodomain transcription factor *Otx2* is expressed

* Corresponding author.
E-mail address: Joseph.Brzezinski@ucdenver.edu (J.A. Brzezinski).

https://doi.org/10.1016/j.ydbio.2019.05.016
Received 7 March 2019; Received in revised form 24 May 2019; Accepted 29 May 2019
Available online 1 June 2019

by a subset of retinal progenitors in their last cell cycle (Muranishi et al., 2011). OTX2 becomes permanently expressed in cells that adopt rod, cone, and bipolar cell interneuron fate (Fossat et al., 2007; Koike et al., 2007). In retinas where *Otx2* is deleted, there are no rods, cones, or bipolar cells. Instead, mutants form excess amacrine cells at the expense of photoreceptors and bipolar cells (Nishida et al., 2003; Sato et al., 2007). Downstream of *Otx2*, the transcription factor *Prdm1* acts in nascent photoreceptors to suppress bipolar cell fate (Brzezinski et al., 2013, 2010; Katoh et al., 2010). Also downstream of *Otx2* is the closely related transcription factor *Crx*, which is necessary for the expression of many photoreceptor-specific genes (Chen et al., 1997; Freund et al., 1997; Furukawa et al., 1999, 1997; Hennig et al., 2008; Hsiau et al., 2007). In contrast to *Otx2* mutants, mice lacking *Crx* still form rod and cone photoreceptors (Blackshaw et al., 2001; Furukawa et al., 1999; Hsiau et al., 2007). While *Otx2*, *Crx*, and *Prdm1* broadly mark developing photoreceptors, the transcription factors *Rxrg* and *Thrb* mark only cones. Mutating *Rxrg* or *Thrb* does not prevent cone formation, but instead affects which types of cone opsin are expressed (Ng et al., 2001; Roberts et al., 2006, 2005; Applebury et al., 2007; Eldred et al., 2018). Taken together, these data suggest a multi-step model of photoreceptor development. First, a subset of retinal progenitors exits the cell cycle and activates *Otx2* expression. Second, the presence of OTX2 imparts these cells with the potential (competence) to adopt rod, cone, and bipolar cell fates. Third, these OTX2+ cells are instructed to adopt either rod, cone, or bipolar fate choice. How these steps are regulated during cone development is poorly understood.

Since cones are rare and form over several days of development in mice (Carter-Dawson and LaVail, 1979; Jeon et al., 1998), we have relatively little power to investigate the gene regulatory networks that control cone development. To overcome these barriers, we sought to create a developmental system where: (1) the fraction of cells that adopt cone fate is greatly increased, and (2) cone development is relatively homogeneous. Combined, these two key features provide power to temporally profile the events that occur in cone development. To create this developmental system, we perturbed the Notch signaling pathway. Prior work has shown that Notch signaling maintains retinal progenitors and suppresses photoreceptor formation (Cau et al., 2019; Eiraku et al., 2011; Geling et al., 2002; Jadhav et al., 2006; Mizeracka et al., 2013; Muranishi et al., 2011; Nakano et al., 2012; Nelson et al., 2007; Perron and Harris, 2000; Riesenberg et al., 2009; Völkner et al., 2016; Yaron et al., 2006). The γ-secretase inhibitor DAPT was initially developed to reduce amyloid-beta peptide levels in the brain, but it also inhibits the cleavage of NOTCH receptors and blocks signal transduction (Panza et al., 2010). Treatment of retinas with DAPT strongly inhibits Notch signaling, quickly forces retinal progenitors out of the cell cycle, and leads to excess neuron production (Nelson et al., 2007). This supernumerary neurogenesis is temporally restricted, showing bias toward the cell types that are normally born at the time of treatment (Nelson et al., 2007; Perron and Harris, 2000; Wall et al., 2009; Kuribayashi et al., 2014). We administered DAPT at the peak of cone genesis (E14.5) (Carter-Dawson and LaVail, 1979) in mouse retinal explants to increase the number of cones formed over a narrow window of time. We observed that DAPT treatment massively increased the number of cones in retinal explants. By conducting histology and bulk RNA-sequencing at multiple time-points, we determined that cone development progressed in a semi-synchronous fashion. From our temporal analysis, we identified many genes whose expression increased upon DAPT treatment. Some of these genes, such as the transcription factors *Ascl1*, *Neurog2*, *Olig2*, and *Mybl1*, preceded *Otx2* expression. These genes may regulate the activation of *Otx2*. Other genes, such as *Meis2*, *Podxl*, and *Vexin* were upregulated after *Otx2* and may instead act as regulators of cone fate specification. We further show that the membrane protein PODXL is expressed specifically within the inner segments of cone photoreceptors. Lastly, we demonstrate that human 3-dimensional (3D) retinal organoids can be made cone dominant by a similar treatment regimen with γ-secretase inhibitors and that this regimen may also accelerate the rate of cone development. Together, our results provide insight into the temporal gene regulatory events that occur both upstream and downstream of *Otx2* as cells adopt cone identity. Further studies will show whether these genes control *Otx2* expression and if they instruct cone fate choice.

2. Results

2.1. γ-secretase inhibitor treatment of E14.5 mouse retinas increases cone photoreceptors at the expense of progenitors

During development, Notch signaling prevents retinal progenitors from prematurely differentiating as neurons, such as cone photoreceptors (Cau et al., 2019; Eiraku et al., 2011; Geling et al., 2002; Jadhav et al., 2006; Mizeracka et al., 2013; Muranishi et al., 2011; Nakano et al., 2012; Nelson et al., 2007; Perron and Harris, 2000; Riesenberg et al., 2009; Völkner et al., 2016; Yaron et al., 2006). Treatment with γ-secretase inhibitors, which disrupt Notch signal transduction, depletes the progenitor pool and induces neurogenesis in a temporally restricted fashion that parallels the birthdating pattern seen for retinal neurons (Nelson et al., 2007; Perron and Harris, 2000; Wall et al., 2009, Kuribayashi et al., 2014). Since cone photoreceptor birthdating peaks around E14.5 in mice (Carter-Dawson and LaVail, 1979), we reasoned that inhibiting Notch signaling at this stage would result in supernumerary cone formation. To test this, we treated E14.5 retinal explants with multiple concentrations of the γ-secretase inhibitor DAPT (Geling et al., 2002; Nelson et al., 2007). Retinas from E14.5 embryos were cultured for 48 h in either DMSO vehicle or nine increasing doses of DAPT (100 nM to 10 μM). One hour prior to harvest, EdU was added to explant cultures to acutely mark cells in S-phase (*i.e.*, progenitors). Explants were collected, sectioned, and stained for EdU, RXRγ (cones), and OTX2 (all photoreceptors) (Fig. S1A) (Fossat et al., 2007; Nishida et al., 2003; Roberts et al., 2005). There was a clear dose-response to DAPT treatment (Fig. S1A). While relatively low concentrations of DAPT were able to significantly (unpaired *t*-test, $P < 0.05$) increase OTX2+ cells compared to DMSO treatment (Fig. S1B), it took a higher dose of DAPT to increase RXRγ+ cones (Fig. S1B). Moreover, it took a DAPT dosage of 2 μM to significantly reduce the number of EdU + cells (Fig. S1). Since 10 μM DAPT treatment showed the most robust and reproducible increase in photoreceptors (Fig. S1B), we used this dosage for subsequent experiments.

To further validate this treatment paradigm, we immunostained explants grown for 48 h in DMSO or 10 μM DAPT with additional progenitor and photoreceptor markers (Fig. 1). Treatment with DAPT resulted in an overt loss of EdU + cells and a strong reduction in the numbers of PAX6+ and SOX2+ retinal progenitors compared to DMSO control explants (Fig. 1B). Since these transcription factors also mark amacrine cells (Cherry et al., 2009; De Melo et al., 2003; Marquardt et al., 2001; Surzenko et al., 2013; Taranova et al., 2006; Walther and Gruss, 1991), we expected there to be a small number of PAX6+ and SOX2+ neurons in DAPT-treated explants (Fig. 1B). In contrast to progenitor markers, we saw a massive increase in the number of OTX2+ photoreceptors and RXRγ+ cones in DAPT treated explants compared to controls (Fig. 1C). PRDM1, a pan-photoreceptor marker directly downstream of OTX2, (Brzezinski et al., 2013, 2010; Chang et al., 2002; Hsiau et al., 2007; Katoh et al., 2010; Mills et al., 2017; Wang et al., 2014), was also strongly increased in DAPT treated explants (Fig. 1C). Taken together, our results show that γ-secretase inhibitor treatment at E14.5 massively increases cone photoreceptor genesis at the expense of retinal progenitors.

2.2. Cone photoreceptor formation is semi-synchronous

DAPT treatment of the developing retina leads to permanent cell cycle exit after only 8 h of treatment (Nelson et al., 2007). This raises the possibility that DAPT-treated progenitors are quickly forced out of the cell cycle and then progressively develop into cones in a predominantly synchronized fashion (Nelson et al., 2007). If true, we expected that gene expression changes would align with the events that occur in cone

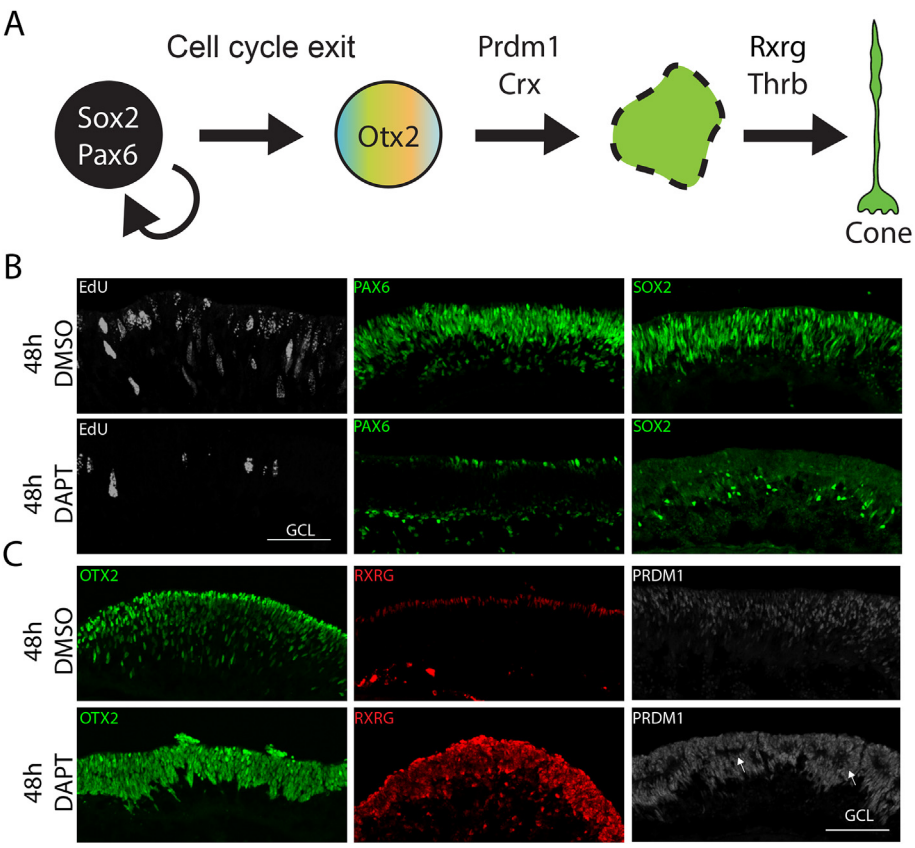

Fig. 1. DAPT treatment at E14.5 leads to supernumerary cone formation and a depletion of progenitors. A. A multi-step model of cone photoreceptor specification showing transcription factor genes that mark different temporal states. B-C. Histological comparison of DMSO control and DAPT treated explants after 48 h of culture. B. Markers for progenitors (EdU incorporation, SOX2, PAX6) are strongly reduced by DAPT treatment. PAX6+ and SOX2+ cells remaining after DAPT treatment likely represent amacrine cells. C. Pan-photoreceptor (OTX2, PRDM1) and cone-specific (RXR_{γ}) markers are greatly increased by DAPT treatment. Arrows point to areas of outer retinal rosetting typically seen after 48 h of DAPT treatment. Scale bars = 50 μm for EdU panels and 100 μm for the remaining panels. GCL = ganglion cell layer.

development (Fig. 1A): (1) retinal progenitors permanently exit the cell cycle, (2) *Otx2* expression is activated to impart photoreceptor competence, (3) cone fate is selected, and (4) cone-specific gene regulatory networks become stabilized (Brzezinski and Reh, 2015). To test this, we treated E14.5 mouse explants with either 10 μM DAPT or DMSO and profiled transcriptional changes at multiple time-points of culturing using a bulk RNA-sequencing methodology (Baird et al., 2014; Bradford et al., 2015; Park et al., 2017) (Fig. 2A). Explants were removed at eleven time-points from 6 h to 48 h of culture, their RNA extracted, and cDNA generated for bulk RNA-sequencing (Fig. 2A). The average gene expression for each treatment was calculated and compared by ANOVA. Gene expression differences within time-points were compared using unpaired t-tests. Genes that were significantly changed between DMSO and DAPT treatment ($P < 0.05$) at one or more culturing time-points were considered for further analysis (Tables S1 and S2). DAPT treatment had a strong effect on gene expression (Fig. 2B); however, these changes were not equivalent across all culturing time-points (Fig. 2B–D). Relatively few genes were differentially expressed after 6 h of DAPT treatment (Fig. 2C), while many genes were divergent by 48 h (Fig. 2D). As expected, Notch target genes such as *Hes1*, *Hes5*, and *Hey1* were decreased after 6 and 48 h of DAPT treatment (Fig. 2C and D). The Notch ligands *Dll1*, *Dll3*, and *Dll4* were rapidly upregulated in response to DAPT treatment (Fig. 2B), as previously described (Nelson et al., 2007). Further Notch pathway component gene expression changes are illustrated in Fig. S2.

Consistent with a developmental progression, transcriptional changes were clustered into four major temporal patterns that we denoted as groups 0–3 (Fig. 2B). We observed that group 0 genes were downregulated at all DAPT treatment time-points (Fig. 2B). Within this group were genes made only by retinal progenitors (*e.g., Fgf15*) and many known Notch signaling targets (*e.g., Hes1, Hey1*). Group 1 genes were transiently increased prior to *Otx2* upregulation, which occurred after ~9 h of DAPT treatment. This group contains genes made in progenitors, such as *Ascl1*, *Neurog2*, and *Olig2* (Fig. 2B, D). Group 2 genes were increased after *Otx2* upregulation, but their elevation was only transient. This group included genes such as *Atoh7* and *Onecut1* (Fig. 2B). The genes in group 3 were activated after *Otx2* and remained expressed throughout the treatment window. Since DAPT-treated explants at 48 h were cone dominant, these group 3 genes presumably mark nascent cones. Indeed, many pan-photoreceptor (*e.g., Crx*, *Prdm1*) and cone-specific (*e.g.*, *Thrb*, *Pdc*, and *Gnat2*) genes were in this group (Fig. 2B, D) (Welby et al., 2017). Overall, these four temporal gene expression groups paralleled the developmental events that occur in cone photoreceptor genesis (Fig. 1A).

If DAPT treatment caused excess cone genesis to proceed in a synchronous fashion, we predicted that we would observe a developmental progression of gene expression changes that matched the sequence of known events in cone formation (Fig. 1A). While this pattern was grossly apparent (Fig. 2B, Tables S1 and S2), we investigated the expression of photoreceptor genes in more detail to establish whether the known temporal order was recapitulated upon DAPT treatment. We observed that *Otx2* became significantly upregulated (unpaired *t*-test; $P < 0.05$) at about 9 h of DAPT treatment (Fig. 2B, Tables S1 and S2). Next, we observed that pan photoreceptor markers *Prdm1* and *Crx* became significantly ($P < 0.01$) upregulated at about 18 and 21 h post-DAPT, respectively (Fig. 2B, Tables S1 and S2). This is consistent with *Prdm1* and *Crx* being regulatory targets of *Otx2* (Brzezinski et al., 2010; Katoh et al., 2010; Mills et al., 2017; Wang et al., 2014). Moreover, this follows the temporal pattern we previously showed by histology where OTX2 expression was activated prior to PRDM1, which was itself activated before CRX (Brzezinski et al., 2010). Downstream of these pan-photoreceptor genes, we observed that early cone-specific factors, such as *Rxrg* and *Thrb* (Ng et al., 2001; Roberts et al., 2006, 2005), became significantly ($P < 0.01$) upregulated after 24 h of DAPT (Fig. 2B, Tables S1 and S2). Cone-specific markers that characterize more mature cones, such as *Gnat2* and *Gngt2* (Welby et al., 2017), were not significantly upregulated until 48 h of DAPT-treatment ($P < 0.01$) (Fig. 2B, Table S1). Considering that gene expression changes occurred in the

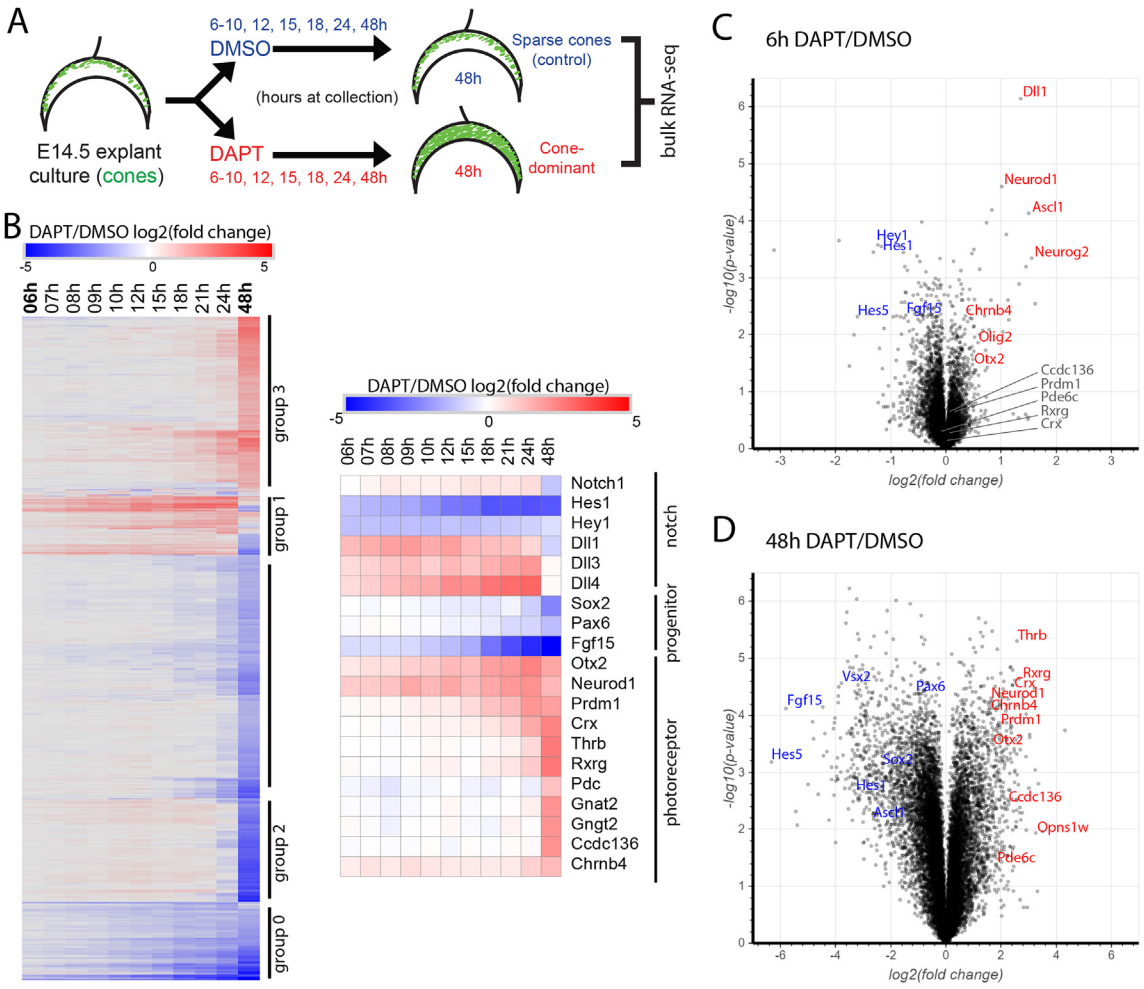

Fig. 2. Temporal patterns of gene expression changes as cells differentiate into cone photoreceptors. A. Schema of DMSO control and DAPT treated explant culturing and time-points for RNA-seq analysis. B. Heatmap of the top 750 differentially expressed genes (blue is downregulated by DAPT and red is upregulated). Upon clustering, they form four conspicuous groups (0 – 3) based on the timing and direction of gene expression changes. The subset of genes on the right side includes markers representing photoreceptors, progenitors, and the Notch pathway. C-D. Volcano plots showing the expression differences between DMSO control and DAPT treated retinas at 6 h and 48 h, respectively. Notable genes are indicated in blue (downregulated) and red (upregulated) text. C. At 6 h of treatment: Notch effector genes (*e.g.*, *Hey1*, *Hes1*, *Hes5*) and progenitor genes (*e.g.*, *Fgf15* and *Vsx2*) are greatly downregulated, while the Notch ligand *Dll1* is upregulated. Transcription factors (*e.g.*, *Neurod1*, *Ascl1*, *Neurog2*, *Olig2*) are upregulated at this early time-point. Photoreceptor genes are generally not differentially expressed (gray) at the earliest treatment time-points. D. At 48 h of treatment, Notch effector genes and progenitor genes are still downregulated. However, there is strong upregulation of pan-photoreceptor (*e.g.*, *Crx*, *Otx2*, *Prdm1*) and cone-specific genes (*e.g.*, *Thrb*, *Rxrg*, *Pde6c*, *Opn1sw*, *Ccdc136*) after 48 h of DAPT treatment.

expected temporal order, it is likely that DAPT treatment synchronized cone development in these explants. However, since proliferative retinal progenitors do not cycle synchronously or uniformly during development (Alexiades and Cepko, 1996; Gomes et al., 2011), it is unlikely that progenitors responded to DAPT treatment with identical timing or kinetics. This suggests that DAPT treatment causes supernumerary cone genesis in a semi-synchronous fashion. Nonetheless, this treatment paradigm still robustly recapitulates the series of events that occur during cone development.

2.3. Gene expression profiling uncovers the temporal events in cone development

It is unknown how a subset of retinal progenitors decide to express *Otx2*, acquire photoreceptor competence, and then become specified as cone photoreceptors. To gain insight into these events, we took advantage of the semi-synchronous nature of cone development in DAPT treated explants. We reasoned that the transcriptional changes that precede *Otx2* upregulation could determine how a subset of progenitors becomes OTX2+ and photoreceptor competent. We further hypothesized that genes activated after *Otx2* would include factors that control cone fate choice within this population. Since a robust cone signature is detected by the end of the DAPT treatment paradigm, we expect that the genes that control cone fate choice and that uniquely mark nascent cones to become differentially expressed prior to 48 h of culture. We further examined a subset of genes in groups 1–3 because their expression changes were consistent with a role in cone genesis.

2.3.1. A small group of genes are transiently expressed prior to Otx2

While the downregulation of genes in group 0 may allow for *Otx2* activation, we instead focused our analysis on transcription factor genes in group 1 that were increased by DAPT treatment prior to the upregulation of *Otx2* at ~9 h (Figs. 2B, 3A). Of note were three basic helix-loop-helix (bHLH) transcription factors (*Ascl1*, *Neurog2*, and *Olig2*) that are made by subsets of progenitors (Brzezinski et al., 2011; Hafler et al., 2012; Hufnagel et al., 2010; Tomita et al., 1996; Jasoni and Reh, 1996). *Ascl1*, *Neurog2*, and *Olig2* are expressed in progenitors with limited proliferative capability or that are in their final cell cycle (Brzezinski et al., 2011; Hafler et al., 2012). Based on this pattern, we expected that DAPT-treated progenitors forced to exit the cell cycle would quickly and

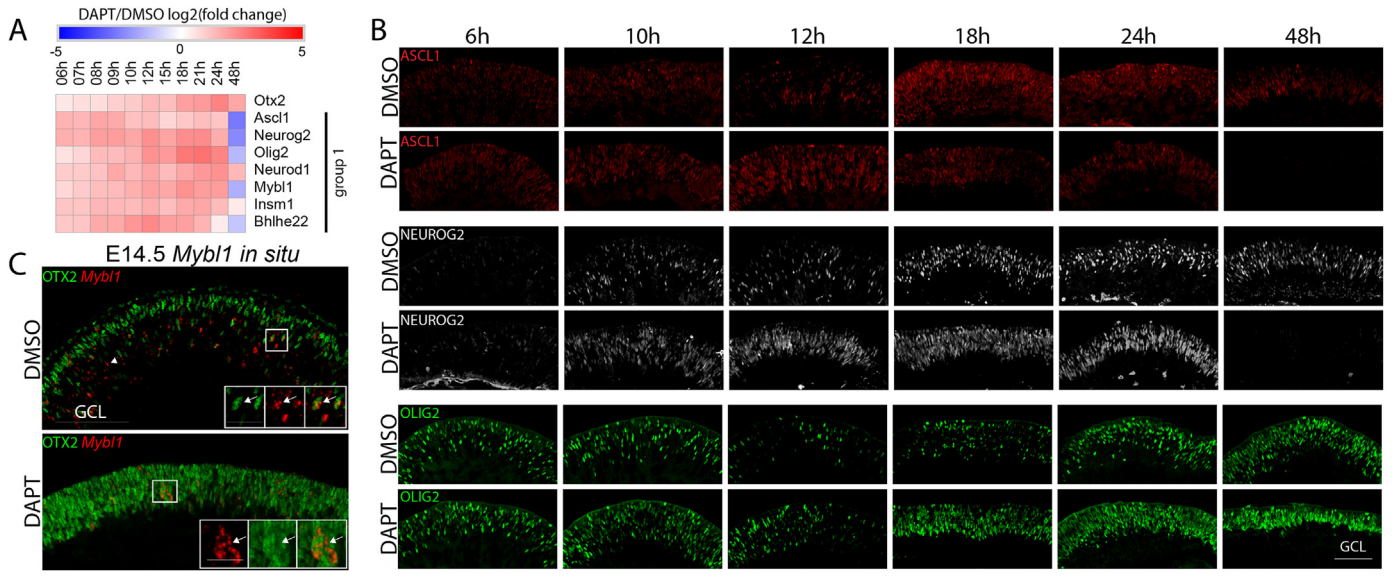

Fig. 3. A small cohort of transcription factors are upregulated in advance of *Otx2*. A. Heatmap of selected transcription factor expression from group 1. These genes are upregulated before *Otx2* (~9 h) and become downregulated after 48 h of DAPT treatment. B. Histological examples of three bHLH family transcription factors (ASCL1, NEUROG2, OLIG2) over the course of treatment. The number of ASCL1+ and NEUROG2+ cells is increased in DAPT treated retinas starting around 6 h, while OLIG2 numbers increase starting around 12 h of treatment. ASCL1 and NEUROG2 labeled cells are nearly absent from DAPT treated retinas by 48 h, while some OLIG2+ cells remain, matching the patterns seen in the heatmap (A). C. RNA *in situ* hybridization for *Mybl1* in DMSO control and DAPT treated retinas. Overlap with OTX2 is seen in both cases (arrows), but is nearly complete following DAPT treatment. The arrowhead marks *Mybl1* signal that does not overlap with OTX2 in the DMSO group. Scale bars = 100 μm for large panels and 25 μm for insets. GCL = ganglion cell layer.

transiently upregulate these factors. We observed that *Ascl1*, *Neurog2*, and *Olig2* expression increased before *Otx2* upregulation (Fig. 3A). Immunostaining for ASCL1, NEUROG2, and OLIG2 showed a salt-and-pepper pattern in DMSO control samples across all time-points (Fig. 3B). DAPT treatment sharply upregulated the number of cells that expressed these transcription factors as early as 6 h of culture (Fig. 3B, Fig. S3). A subset of OTX2+ cells co-expressed ASCL1 and NEUROG2 in both DMSO and DAPT treated explants (Fig. S3). This argues that ASCL1+ and/or NEUROG2+ progenitors directly give rise to OTX2+ cells. Since *Ascl1*, *Neurog2*, and *Olig2* are made by progenitors, we expected their expression to decrease after protracted DAPT treatment. By 48 h, ASCL1+ and NEUROG2+ cells were nearly absent from DAPT treated retinas, matching the transcriptional analysis (Figs. 3A, 3B, S3). OLIG2 staining showed a less dramatic decrease after 48 h of DAPT treatment, but this was consistent with the RNA-seq data (Figs. 3A, 3B, S3). Next, we examined the expression pattern of the transcription factor *Mybl1*. Using RNA *in situ* hybridization in untreated wild-type E14.5 retinal sections, we observed a salt-and-pepper pattern of *Mybl1* expression (Fig. 3C). A subset of *Mybl1*+ cells were co-labeled with antibodies to OTX2 (Fig. 3C). In E14.5 explants treated with DAPT for 24 h, *Mybl1 in situ* signal overlapped nearly completely with OTX2 (Fig. 3C). Similar to what we observed with ASCL1, NEUROG2, and OLIG2, our data suggest that *Mybl1* is made by a subset of retinal progenitors that give rise to OTX2+ cells.

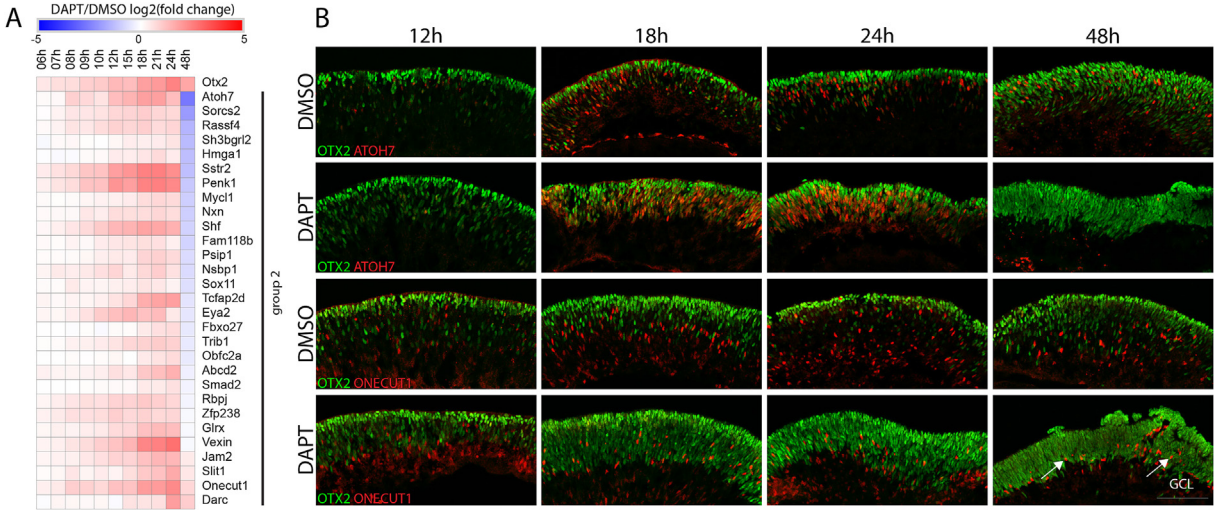

Fig. 4. Several genes are upregulated after *Otx2*, but are only transiently expressed. A. Heatmap of genes from group 2 that increase in DAPT treated retinas after *Otx2* (~9 h). B. Immunohistochemistry showing the expression of ATOH7 and ONECUT1 in comparison to OTX2 in DMSO control or DAPT treated explants at 12, 18, 24, and 48 h time-points. ATOH7 and ONECUT1 expression peaks around 18 h post-DAPT treatment. ATOH7 expression is lost by 48 h while ONECUT1 is limited to horizontal or ganglion cells (OTX2-negative, arrows), matching the expression seen in the heatmap (A). Scale bars = 100 μm for all panels. GCL = ganglion cell layer.

2.3.2. Several genes are transiently activated following Otx2

To understand the developmental events that occur after *Otx2* upregulation, we examined genes in group 2. These genes were upregulated shortly after *Otx2* activation, but decreased by 48 h of DAPT treatment (Figs. 2B, 4A). This pattern is consistent with genes that become activated in cells that just stopped dividing. Moreover, this transient pattern suggests that these genes play a switch-like role in development. Among this group are the well-characterized *Atoh7* and *Onecut1* transcription factors (Fig. 4A). ATOH7 is primarily made in newly postmitotic cells and is required for ganglion cell competence (Brown et al., 2001; Brzezinski et al., 2012; Kay et al., 2001; Wang et al., 2001; Yang et al., 2003). In DMSO-treated explants, ATOH7 expression showed a salt-and-pepper distribution in the retina that partially overlapped with OTX2 (Fig. 4B). This is consistent with prior lineage tracing data that showed that the majority of ATOH7+ cells adopt photoreceptor identities (Brzezinski et al., 2012). DAPT treatment increased *Atoh7* expression starting around 18 h of culture (Figs. 4A and S4). Correspondingly, we observed an increase in the number of ATOH7+ cells histologically, which peaked between 18 h and 24 h of DAPT treatment (Figs. 4B and S4). ATOH7 overlapped with OTX2 at these time-points (Fig. 4B), but by 48 h of DAPT treatment ATOH7+ cells were nearly absent (Figs. 4B and S4). This closely matched what was observed by RNA-seq (Fig. 4A). Similar to ATOH7, ONECUT1 marks a complex population of cells during development. This includes horizontal cells, ganglion cells, and some OTX2+ cells (Emerson et al., 2013; Sapkota et al., 2014; Wu et al., 2013, 2012). *Onecut1* has also been shown to activate the cone-specific marker *Thrb* (Emerson et al., 2013; Sapkota et al., 2014). *Onecut1* expression changed similarly to *Atoh7* in DAPT-treated retinas (Fig. 4A). ONECUT1 partially overlapped with OTX2 in DMSO control and DAPT treated explants at all time-points (Fig. 4B). However, by 48 h of DAPT treatment there were fewer ONECUT1+ cells and they rarely co-expressed OTX2 (Fig. 4B). This is consistent with prior data showing that ONECUT1 expression is transient in a subset of developing OTX2+ cells (Emerson et al., 2013). Several other genes with similar mRNA expression profiles, such as *Vexin*, *Psip1*, and *Sstr2*, remain to be examined as tools become available.

Some of the group 2 genes are unlikely to positively influence cone development. For example, *Sox11* and *Tcfap2d* are transcription factors made by ganglion cells and amacrine cells, respectively (Bassett et al., 2007; Jiang et al., 2013). While cones are overwhelmingly increased upon DAPT treatment, it is likely that other early born fates like horizontal, amacrine, and ganglion cells are modestly increased. We stained explants with AP2B (amacrine & horizontal cells) and pan-BRN3 (ganglion cell) antibodies (Fig. S5B) (Xiang et al., 1995; Bassett et al., 2012). In contrast to our prediction, we observed significantly fewer AP2B+ and BRN3+ cells ($P < 0.001$) after 48 h of DAPT treatment compared to DMSO controls (Fig. S5B). We next co-stained DAPT-treated explants cultured for 48 h with PAX6 (amacrines, horizontals, & ganglion cells), LHX1 (horizontal cells) and OTX2 (De Melo et al., 2003; Liu et al., 2000; Marquardt et al., 2001). The PAX6+ and LHX1+ populations did not overlap with OTX2+ photoreceptors (Fig. S5A). Similarly, AP2B was rarely, if ever, co-expressed with the cone marker RXRγ (Fig. S5B). A few cells were seen that co-expressed AP2B and BRN3, but this overlap was not increased by DAPT treatment (Fig. S5B). These data suggest that DAPT treated explants form a limited number of amacrines, horizontals, and ganglion cells, but do not co-express definitive markers of multiple identities simultaneously.

Since we did not observe the expected increase in other retinal neuron types born at E14.5, we reasoned that some cells were dying from the DAPT treatment. We also expected there to be elevated ganglion cell death because these cells do not receive trophic support from their brain targets in explants (Meyer-Franke et al., 1995). We stained for activated caspase 3 (AC3) to mark apoptotic cells and observed considerable cell death in the ganglion cell layer (Fig. S7A). When we quantified AC3+ cells outside of the ganglion cell layer, we observed significantly ($P < 0.01$) elevated cell death in DAPT treated retinas compared to controls at both 6 and 48 h of treatment (Fig. S7A). These results suggest that DAPT treatment increases cone and other retinal neuronal cell death.

2.3.3. A large subset of genes are expressed following Otx2, remain expressed, and may contribute to cone photoreceptor identity and function

Similar to group 2, the genes in group 3 were upregulated after *Otx2* activation (Figs. 2B, 5A). However, these genes remained upregulated after 48 h of DAPT treatment. Most of the group 3 genes were only significantly upregulated at the 48 h treatment time-point. This included numerous cone-specific genes, such as *Arr3*, *Gnat2*, *Pde6c*, *Gngt2*, *Opn1sw*, and *Ccdc136* (Figs. 1C, 2C, Table S1) (Corbo et al., 2007; Smiley et al., 2016; Welby et al., 2017). A small subset of group 3 genes became upregulated prior to 48 h. These could represent cone fate choice regulators and includes genes with known roles in photoreceptor development, such as *Prdm1*, *Crx*, *Thrb*, and *Rxrg* (Figs. 1C, 2B and 2D, 5A). We further examined two of these genes (*Podxl* and *Meis2*) that were first significantly upregulated after 24 h of DAPT treatment ($P < 0.01$) (Fig. 5A).

PODXL (Podocalyxin-like) is a membrane protein found in podocytes of the kidney and within vascular endothelial cells (Chen et al., 2004; Doyonnas et al., 2005; Kerjaschki et al., 1984). We stained DMSO and DAPT treated retinal explants using antibodies specific to PODXL (Kang et al., 2017). In 24 h DMSO and DAPT treated explants, PODXL staining strongly labeled the apical surface of cells on the scleral side of the retina (Fig. 5B). After 48 h of DAPT treatment, the area of PODXL staining was increased, mirroring the gene expression data (Fig. 5A and B). We then co-stained wild-type E14.5 retinal sections with RXRγ and PODXL (Fig. 5C). PODXL stained the apical portion of the retina intensely and labeled some hyaloid vessels abutting the inner retinal surface (Fig. 5C). Low intensity PODXL staining surrounded RXRγ+ cells, suggesting that this is an early cone-specific marker in the retina. Since group 3 genes remain expressed at end of the treatment period, we reasoned that *Podxl* would be expressed by mature cones. Therefore, we stained adult wild-type retinal sections for PODXL and cone-specific markers (RXRγ, ARR3, and OPN1MW) (Fig. 5C) (Kühn, 1978; Wilden et al., 1986). RXRγ staining in the outer retina is specific for cones. We observed strong PODXL staining immediately adjacent to RXRγ+ cones (Fig. 5C). Co-staining with ARR3 (cone arrestin) showed that PODXL marked all cone photoreceptors, but that it was localized to only a subdomain of the cell (Fig. 5C). We then stained sections for M-opsin (OPN1MW), which preferentially marks the outer segment of many mouse cones. PODXL staining overlapped poorly with M-opsin and was localized closer to the cell body (Fig. 5C). This pattern is consistent with PODXL marking the inner segments of cone photoreceptors in the adult retina. In all sections, PODXL stained the retinal and choroidal vasculature systems (Fig. 5C). Taken together, our data suggest that PODXL is an early marker of developing cone photoreceptors.

We then examined the expression of the homeodomain transcription factor *Meis2* by RNA *in situ* hybridization. In E15.5 wild-type retinal sections, *Meis2* was detected in a small number of cells localized towards the outer portion of the retina (Fig. 5D). The *Meis2* signal overlapped extensively with OTX2 (Fig. 5D). This suggests that *Meis2* is expressed by a subset of OTX2+ cells. We were unable to determine whether *Meis2* expression is cone-specific as the *in situ* hybridizations were incompatible with our cone markers. Although *Meis2* remains upregulated at 48 h, we were not able to detect signal in adult cones (data not shown). Recently, *Meis2* has been described in the adult retina, where it marks OFF-type retinal ganglion cells (Peng et al., 2019). Therefore, *Meis2* may only be transiently expressed within a subset of developing photoreceptors. As described above, some genes in group 3 appear to mark other neuronal populations. For example, the increase in *Neurod4* is likely marking amacrine cells (Inoue et al., 2002). We also noted a small, but significant ($P < 0.01$) increase in some rod photoreceptor genes, such as *Nrl and Samd7*, after 48 h of DAPT treatment (Fig. 5A, Table S1) (Akimoto et al., 2006; Hlawatsch et al., 2013; Mears et al., 2001; Omori et al., 2017).

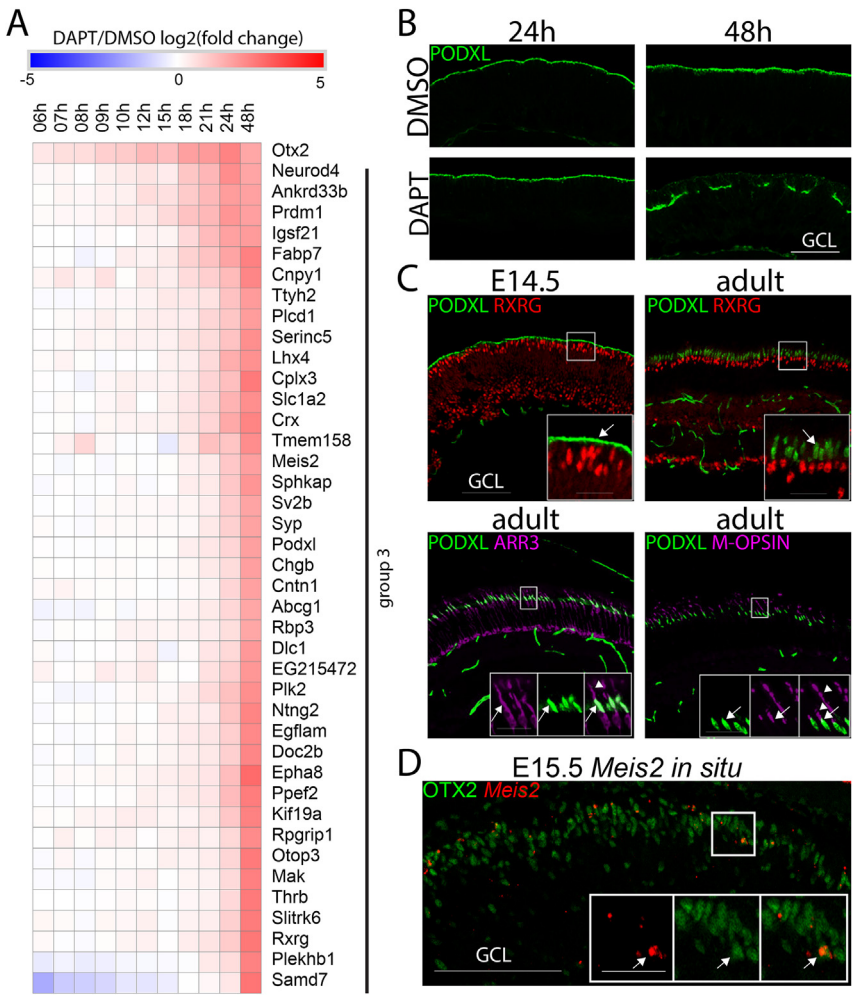

Fig. 5. Many genes are upregulated after *Otx2* and remain expressed. A. Heatmap for genes in group 3 that remain upregulated after 48 h of DAPT treatment. This includes many genes made by cones, such as *Rxrg* and *Thrb*. B-C. Immunostaining for PODXL, a known membrane protein. B. PODXL staining in E14.5 explants treated for 24 or 48 h with either DMSO or DAPT. PODXL staining is localized to apical portion of the nascent photoreceptor layer and reveals the outer retinal rosetting that occurs in explants treated with DAPT for 48 h. C. PODXL expression in untreated retinas at E14.5 and in adults relative to the cone markers RXRγ, ARR3, and M-Opsin. At E14.5, PODXL is ubiquitous along the apical membrane (arrow) of the photoreceptor layer and it is difficult to distinguish whether expression is cone-specific (RXRγ+). In the adult retina, PODXL expression marks the vasculature and a subdomain of photoreceptors. Arrows point to localization of PODXL relative to RXRγ, ARR3, or M-Opsin staining. PODXL is localized apically in a one-to-one ratio with RXRγ (arrow). All of the cone arrestin (ARR3) positive cells co-express PODXL, but only in a subdomain of the cone (arrows) that is consistent with the inner segment region. Arrowheads mark the outer segment area. M-Opsin staining marks the outer segment (arrowheads) of most mouse cones and this staining was distal to the PODXL signal (arrows). Together, this suggests that PODXL is cone-specific and localized to only the inner segment region of cones. D. RNA *in situ* hybridization for *Meis2* at E15.5. At this stage, *Meis2* signal overlaps extensively with OTX2 (arrows), but only a subset of OTX2+ cells co-express *Meis2*. Scale bars = 100 μm for panels within B, C, & D and 25 μm for insets. GCL = ganglion cell layer.

2.4. Human 3D retinal organoids can be programmed to a cone-biased state

Since the γ-secretase inhibitor DAPT increased cones in mouse retinal explant cultures, we reasoned that human 3D retinal organoids would respond similarly. In the human retina, cones are formed over a longer developmental window than in mice. There are also large regional differences in the timing of development, such that neurons near the fovea are formed weeks before those in the peripheral-most retina (Hendrickson et al., 2012; Hendrickson and Yuodelis, 1984; Hoshino et al., 2017). In human 3D retinal organoids, pan-photoreceptor markers like CRX and RECOVERIN are seen by 6 weeks of culture (Gonzalez-Cordero et al., 2017; Zhu et al., 2018). Since the first photoreceptors formed are cones, this suggested that 6 week human retinal organoids were capable of generating cones. Thus, we tested whether γ-secretase inhibitors could massively increase cone photoreceptor formation in 6 week human organoids.

Human retinal organoids derived from iPSCs were grown in culture for 6 weeks and then treated with DMSO vehicle or DAPT for an additional 3 days. While DAPT was able to promote cone formation, its effects were highly variable in our experiments (data not shown). Therefore, we used the γ-secretase inhibitor PF-03084104 (PF-4014) (10 μM) instead of DAPT (Fig. 6A). PF-4104 is similar in function to DAPT and acts as a non-transition state γ-secretase inhibitor (Olsauskas-Kuprys et al., 2013). It is a potent Notch signaling inhibitor and may have less off-target sensitivity (Wei et al., 2010). Control and PF-4014 treated retinal organoids were sectioned and stained with progenitor and photoreceptor-specific markers. Ki67 and VSX2 progenitor staining was robust in controls, but these markers were essentially absent from PF-4014 treated organoids, consistent with a loss of retinal progenitors (Fig. 6B, C). Similar to what is seen in DAPT-treated mouse explants (Figs. 3B, 4B), ATOH7 and ASCL1 expression were severely decreased in organoids treated with PF-4014 (Fig. 6B, C). Like treated mouse explants, there was a massive increase in the number of cells expressing photoreceptor markers upon treatment with PF-4014 (Fig. 6B, C). Cells that expressed the pan-photoreceptor markers OTX2, CRX, and PRDM1 were increased by PF-4014 treatment versus controls (Fig. 6B, C). The cone markers RXRγ and ARR3 were sparsely detected in untreated control organoids (Fig. 6B). In contrast, PF-4014 treated organoids had considerably more RXRγ+ and ARR3+ cones (Fig. 6B, C). Since PF-4014 treatment may increase other early-born neurons, we examined these organoids for ganglion cells with antibodies against BRN3A (Fig. S6C). Unlike mouse explants, we saw a modest yet significant increase ($P < 0.01$) in BRN3A+ ganglion cells after PF-4014 treatment (Fig. S6C'). We next assayed cell death in the organoids using a terminal deoxynucleotidyl transferase dUTP nick end labeling (TUNEL) assay (Fig. S7B). Unlike DAPT-treated mouse explants, we observed no increase in TUNEL+ dying cells between control and PF-4014 treated organoids (Fig. S7B). Taken together, γ-secretase inhibitor treatment of human organoids can cause supernumerary cone genesis and largely recapitulates what is seen in mice at a similar developmental stage.

3. Discussion

The gene regulatory networks that govern cone photoreceptor development are largely unknown. Here we used γ-secretase inhibitor

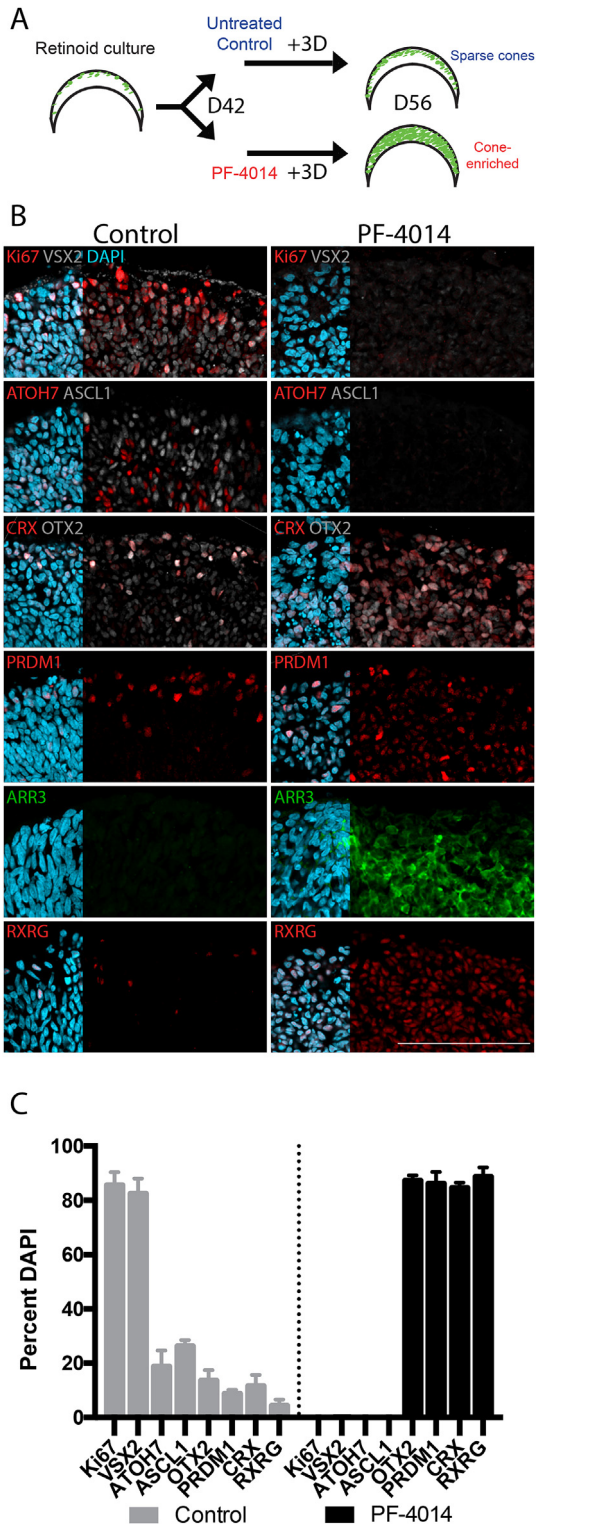

Fig. 6. Supernumerary cone formation occurs in human retinal organoid cultures. A. Schema of human cone enrichment in retinal organoid culture after treatment for three days (+3D) with either water vehicle or the γ-secretase inhibitor PF-4104. Organoids were treated on day 42 and examined by histology on day 56. B. Human retinal organoids immunostained with markers for progenitors (Ki67, VSX2, ASCL1, ATOH7), photoreceptors (OTX2, CRX, PRDM1), and specifically for cones (ARR3, RXRγ). Similar to mouse E14.5 explants, there is a significant loss of progenitor markers (Ki67, VSX2, ASCL1, ATOH7) following PF-4014 treatment. As expected, PF-4014 treatment results in a strong upregulation of pan-photoreceptor markers (CRX, OTX2, PRDM1). The number of cells expressing the cone-specific markers RXRγ and ARR3 is greatly increased by PF-4014 treatment. PF-4014 may advance the timing of ARR3 expression, as it was not appreciably present in DMSO-treated organoids at day 56. Scale bars = 100 μm for all panels. GCL = ganglion cell layer. C. Quantification of selected marker expression compared to DAPI. Error bars represent the SD.

(caption on next column)

treatment to semi-synchronize cone development. From this, we were able to use histology and RNA-seq to temporally map the transcriptional events that occur during cone formation. This confirmed known regulatory genes and revealed several novel genes that may regulate cone photoreceptor fate specification and function. Our analysis provides a foundation for further studies to determine how these novel genes control cone development.

3.1. Treating with γ-secretase inhibitors semi-synchronizes cone development

Several experiments have shown that blocking Notch signaling genetically or with γ-secretase inhibitors can increase retinal neuron formation (Cau et al., 2019; Eiraku et al., 2011; Geling et al., 2002; Jadhav et al., 2006; Mizeracka et al., 2013; Muranishi et al., 2011; Nakano et al., 2012; Nelson et al., 2007; Perron and Harris, 2000; Riesenberg et al., 2009; Völkner et al., 2016; Yaron et al., 2006). The types of neurons that are increased depends on the stage of development that Notch signaling is blocked (Nelson et al., 2007; Perron and Harris, 2000; Wall et al., 2009, Kuribayashi et al., 2014). We show that using γ-secretase inhibitors at E14.5 in the mouse, the peak of cone genesis, leads to a massive increase in cones. Similarly, we show that γ-secretase inhibitor treatment of human iPSC-derived organoids at 6 weeks of culture greatly increased cone genesis. RNA-seq and histology revealed that regulators of mouse cone development were upregulated in their previously known temporal order. Since mouse progenitors are heterogeneous (Alexiades and Cepko, 1996; Gomes et al., 2011) and we used a bulk RNA-sequencing approach that will average-out gene expression changes, the clear temporal order we see strongly indicates that cone development has been synchronized by DAPT treatment. Because DAPT is unlikely to have differentiated all cells with the same timing or rate, we suggest that γ-secretase inhibitor treatment acts to semi-synchronize cone development. Nonetheless, this is sufficient to infer a temporal order of developmental events in cone genesis (see below). While there was a massive increase in cones, we also detected signatures of other cell types by the end of the DAPT treatment (Table S1). This is not unexpected as the genesis of these cell types also occurs at E14.5 (Rapaport et al., 2004; Young, 1985).

3.2. Temporal analysis of gene expression reveals genes that may control unique aspects of cone development

Our analysis of gene expression changes between control and DAPT treated mouse explants recapitulated the events that are thought to occur in photoreceptor development (Fig. 1A) (Brzezinski and Reh, 2015). In order, we saw that: (1) retinal progenitor genes were downregulated, (2) genes marking cells in their terminal cell cycle (*i.e.*, neurogenic or proneural) became transiently upregulated, (3) *Otx2* was upregulated, (4) pan-photoreceptor genes become upregulated, (5) cone-specific genes were upregulated, and finally (6) mature cone marker genes were

activated. To better understand genes whose roles are unknown in cone development, we grouped them into four broad groups based on the direction, timing, and permanence of their expression changes upon DAPT treatment.

Genes in group 0 were downregulated throughout the treatment period. The known genes in this group mostly represented progenitor-specific and Notch pathway related genes. While beyond our current investigation, these genes may directly repress *Otx2*. Downregulating group 0 genes may "release" cells, enabling them to adopt neuronal identities. In contrast, genes upregulated prior to *Otx2* may directly activate its expression. To find such factors we focused on group 1 genes, which became transiently upregulated by DAPT treatment prior to *Otx2* activation. These genes may activate *Otx2* and establish the population of cells that are competent to form rods, cones, and bipolar cells. Of particular interest in this group were the transcription factors *Ascl1*, *Neurog2*, *Olig2* and *Mybl1*. ASCL1, NEUROG2, and OLIG2 are expressed in retinal progenitor cells, albeit in a heterogeneous partially overlapping pattern (Brzezinski et al., 2011). Overexpression of these factors can have a proneural effect and drive progenitors out of the cell cycle (Bertrand et al., 2002). We observed that some OTX2+ cells in controls and DAPT treated explants co-expressed these transcription factors. Consistent with an activating role, *Ascl1* overexpression in Müller glia was able to turn on *Otx2* expression (Pollak et al., 2013). Nonetheless, individual knockouts of these three genes have only modest effects on photoreceptor development (Brzezinski and Reh, 2015). *Ascl1*-null mice are able to form cone photoreceptors (Tomita et al., 1996). *Neurog2* mutants show no effect on cone formation and a just mild phenotype on the numbers of rods and bipolar cells that are generated (Hufnagel et al., 2010; Kowalchuk et al., 2018). *Olig2* loss has no effect on retinal cell populations (Hafler et al., 2012). Taken together, these findings suggest that there is redundancy or compensation that occurs between these factors during development. The transcription factor *Mybl1* showed a similar transcriptional pattern to *Ascl1*, *Neurog2*, and *Olig2* and co-localized with OTX2. How *Mybl1* controls retinal development is unknown, but it has been shown to regulate meiosis during spermatogenesis (Bolcun-Filas et al., 2011). *Mybl1* is similar to two other genes expressed in the retina (*Myb*, *Mybl2*) (Tables S1–3) and may also act in a redundant or compensatory fashion to regulate *Otx2* and photoreceptor development. Future experiments where multiple transcription factors are simultaneously mutated will overcome these barriers and reveal whether group 1 genes regulate cone genesis.

Genes in group 2 were transiently upregulated by DAPT treatment after *Otx2*. Group 2 genes may act like switches downstream of *Otx2* to select fate choices within this population of cells. In this group were two previously characterized genes, *Atoh7* and *Onecut1*. *Atoh7* is required for ganglion cell formation and cells expressing this factor are competent to adopt other fates, such as rod and cone photoreceptors (Brown et al., 2001; Brzezinski et al., 2012; Kay et al., 2001; Wang et al., 2001; Yang et al., 2003). Thus, it is unlikely that *Atoh7* controls fate choice in OTX2+ cells, but instead acts permissively and transiently marks cells that will become cones. *Onecut1* is normally expressed by a subset of OTX2+ cells and can activate cone-specific gene expression (Emerson et al., 2013). However, double mutants of *Onecut1* and *Onecut2* do not totally prevent cone genesis in the mouse (Sapkota et al., 2014). This raises the possibility that redundant and/or compensatory mechanisms mask whether *Onecut1* controls cone fate specification. Several other group 2 genes may influence cone fate specification and remain to be investigated. Of particular interest is the gene *3110035E14Rik*, now referred to as *Vexin*. This gene has been identified as a neurogenic factor that may cooperate with bHLH transcription factors to modulate their developmental effects (Moore et al., 2018). Moore and colleagues showed that both overexpression and knockdown of *Vexin* in *Xenopus* affected photoreceptor genesis at the expense of other retinal cell types (Moore et al., 2018). They also found that *Vexin* works through a cyclin dependent kinase inhibitor to increase *Neurog2* and promote neurogenesis (Moore et al., 2018). How genes in groups 1 and 2 interact with each other and *Otx2* to control cone development remains to be determined.

The largest category of gene expression changes showed upregulation after *Otx2* and had sustained activation after 48 h of DAPT treatment. These group 3 genes included pan-photoreceptor transcription factors such as *Crx* and *Prdm1* along with cone-specific factors like *Thrb* and *Rxrg*. Many other known cone-specific genes are in this group, but most of these were not upregulated until 48 h of DAPT treatment. Of particular interest were genes whose expression was upregulated around the time of *Thrb* and *Rxrg* at ~24 h of DAPT treatment. While both of these factors mark cones, neither are necessary for cone genesis. Instead, they control cone subtype (M versus S) choice (Ng et al., 2001; Roberts et al., 2006, 2005; Applebury et al., 2007; Eldred et al., 2018). One transcription factor that became upregulated with similar timing was *Meis2*, which showed near complete overlap with OTX2. We were unable to determine whether *Meis2* marks the subset of OTX2+ cells that adopt cone identity for technical reasons. We did not detect *Meis2* in adult cones, suggesting that any role it plays in cone development is transient. Another factor with a similar expression pattern is *Podxl* or Podocalyxin-like, a transmembrane protein first identified as an anti-adhesion glycoprotein molecule similar in structure and function to the well characterized CD34 (Sassetti et al., 1998). It is expressed in the kidney, the vascular system, and within the developing nervous system (Ney et al., 2007; Siemerink et al., 2016; Vitureira et al., 2010, 2005; Zhang et al., 2019). Loss of *Podxl* is perinatal lethal and has been shown to cause axonal and synaptic deficits in the central nervous system (Vitureira et al., 2010). We found that PODXL marks developing photoreceptors, though it was difficult to determine whether this was cone-specific due to its localization in apical membranes. Nonetheless, we observed that PODXL specifically marked cone inner segments in the adult mouse retina. Other gene expression profiling experiments have detected *Podxl,* with some attributing it to rods, cones, or both (Hughes et al., 2017; Lakowski et al., 2011; Welby et al., 2017). The reasons for these disparities are unclear, though our immunostaining data argues in favor of cone-specific expression in the mature retina (Fig. 5C). It is unclear what role PODXL plays during cone development and homeostasis. One possibility is that PODXL has an anti-adhesive role and keeps cones from clumping together. Conditional *Podxl* knock-out mice will be needed to ascertain its role in cones, both to escape lethality and to avoid its potentially confounding roles in the ocular vasculature.

3.3. Using γ-secretase inhibitors to increase and accelerate human cone development

We and others have seen that γ-secretase inhibitors can increase the formation of cone photoreceptors in human 3D organoid cultures (Nakano et al., 2012). We saw a very robust increase in cone-specific markers when we treated 6-week human organoids with the γ-secretase inhibitor PF-4014. Prior work has shown an increase in human cones with DAPT treatment, but this was done with slightly earlier timing and did not result in as robust of an effect (Nakano et al., 2012). In our experiments, PF-4014 was much more effective than DAPT. While PF-4014 is thought to be slightly more effective at inhibiting Notch signaling than DAPT (Wei et al., 2010), it remains unclear why there was a difference as we used relatively high doses of both compounds in our experiments. One possibility is that PF-4014 had better delivery properties than DAPT, reaching cells in the 3D organoids more effectively. The differences in cell death and ganglion cell numbers between mouse and human retinas suggests that PF-4014 has less toxicity than DAPT. Alternatively, mouse and human cells may respond slightly differently to these drugs. The cells could also be at a modestly different developmental stage or competence state at the time of treatment. Regardless of the mechanism, the use of PF-4014 on 6-week human organoids may be a highly effective method for generating large numbers of cones for developmental studies, drug screens, or for cell transplantation experiments. We also observed that ARR3 expression was strongly upregulated by PF-4014, but was essentially absent from control organoids. This raises the possibility that

γ-secretase inhibitor treatment accelerates the developmental timing of cone genesis. The large number of known cone-specific genes seen in 48 h DAPT treated E14.5 retinal explants suggests that this may occur in the mouse system as well. Moving forward, single-cell RNA-sequencing approaches can be used to test whether cone development is accelerated by γ-secretase inhibitors. Accelerating human cone genesis has the potential to facilitate drug screening assays and cell transplantation experiments by greatly shortening organoid culturing times.

4. Methods

4.1. Murine retinal explant culture and immunostaining

All animal experiments were conducted in accordance with the University of Colorado Denver IACUC guidelines. Embryonic day 14.5 wild-type *CD1* embryos (strain #022, Charles River Laboratories, Wilmington, MA) were used for retinal explant cultures. Both eyes were removed and placed in cold Hank's Balanced Salt Solution (HBSS with Ca2+ and Mg2+) (Corning, Corning, NY, USA) containing 6 mg/mL glucose and 0.05 M HEPES. The eyes were further dissected leaving only the retina and lens intact. These were kept on ice in growth media, which consisted of Neurobasal Medium containing 1X N2 supplement, 1X L-glutamine, 1X Penicillin/Streptomycin, and 1% Fetal Bovine Serum (FBS) (Gibco/Thermo Fisher Scientific, Waltham, MA, USA) until ready for subsequent experimental incubations (Mills et al., 2017). Three to four retinas per treatment were placed into a single well of a 24-well plate containing growth media with either 10 μM DAPT (565770, Calbiochem Milipore Sigma, Burlington, MA, USA) or the equivalent volume of DMSO vehicle (1 part in 1000). The explants were grown under 5% CO_2 in a 37°C incubator using a nutator (at 12 RPM) to gently mix them for 6, 8, 10, 12, 18, 24, or 48 h. After culture, explants were fixed in 2% paraformaldehyde for 20 min, passed through a sucrose gradient (at 10% & 20% for 30 min and 30% overnight) and frozen in OCT medium (Sakura, Torrance, CA, USA). Sections were cut at 10 μm and placed on slides for immunohistochemistry (Brzezinski et al., 2010). Briefly, slides were incubated at room temperature for 1 h in milk block solution (the supernatant of 5% milk and 0.5% Triton X-100 in Phosphate Buffered Saline (PBS)). Primary antibodies diluted in milk block were incubated overnight for 12 to 18 h on slides, which were then washed in PBS. Sections were then incubated for 1 h at room temperature with fluorescently conjugated secondary antibodies (Jackson ImmunoResearch, West Grove, PA, USA) diluted 1:500 in milk block solution. Images were acquired using a Nikon C2 laser scanning confocal microscope (Melville, NY, USA). A 1024 × 1024 pixel photograph was captured for each of the retinal sections using each laser sequentially to generate the final image. Three to five z-stacks (1–1.5 μm per slice) were captured, maximum-intensity Z-projected with ImageJ (Schneider et al., 2012) and minimally processed in Adobe Photoshop CC 2015 (Adobe, San Diego, CA, USA). Primary antibodies used: rabbit anti-AC3 (1:250) (5559565, Becton Dickinson, Franklin Lakes, NJ, USA) rabbit anti-AP2B (1:250) (SC8976, Santa Cruz Biotechnology, Santa Cruz, CA, USA), mouse anti-ASCL1 (1:250) (556604 BD Pharmingen, San Jose, CA, USA) or guinea pig anti-ASCL1 (1:1000, gift from J. Johnson, UT Southwestern), rabbit anti-ARR3 (1:250) (AB15282, Millipore, Burlington, MA, USA), rabbit anti-ATOH7 (1:500) (NBP1-88639, Novus, St. Charles, MO, USA), goat anti-BRN3 (1:250) (sc-6026, Santa Cruz), rabbit anti-M-OPSIN (1:250) (AB5405, Millipore), mouse anti-NEUROG2 (1:250) (MAB3314, Santa Cruz Biotechnology, Santa Cruz, CA, USA), rabbit anti-OLIG2 (1:250) (AB9610, Millipore), rabbit anti-ONECUT1 (1:250) (sc-13050, Santa Cruz), goat anti-OTX2 (1:250) (BAF1979, R&D, Minneapolis, MN, USA), rabbit anti-PAX6 (1:250) (901301, Biolegend, San Diego, CA, USA), goat anti-PODXL (1:1000) (AF1556, R&D), rat anti-PRDM1 (1:250) (AA235-395, Santa Cruz), rabbit anti-RXR_γ (1:250) (sc-555, Santa Cruz), goat anti-SOX2 (1:250) (sc-17320, Santa Cruz). Visualization of EdU incorporation was performed using the Click-iT™ EdU Imaging Kit (C10337, Thermo Fisher). Immunostaining quantification was performed using captured images from above. Image stacks were imported into ImageJ and channels normalized. Manual cell counts were made in each channel and recorded in Microsoft Excel (Microsoft, Redmond, WA, USA). Cell counts were acquired from images and normalized to 250 μm of retinal length or per 200X field. Unpaired t-tests were performed using Excel or GraphPad Prism 6 (GraphPad, San Diego, CA, USA) and P-values less than 0.05 were considered to be significant.

4.2. Adult murine tissue collection

For comparative analysis, adult eyes were acquired from *CD1* (Charles River) female mice at the time of embryo harvest (above). Corneas were punctured with a 30g needle and eyes were fixed in 2% paraformaldehyde. Whole eyes then were incubated in 10% & 20% sucrose for 1 h each and 30% sucrose overnight. Tissue was then frozen in OCT, sectioned at 10 μm, and stained and imaged as above.

4.3. Mybl1 and Meis2 in situ hybridization

Retinal tissue was harvested from *C57*BL*/6J* mice (strain #0664) (Jackson Laboratories, Bar Harbor, ME, USA) as described above at E14.5 or E15.5. RNA *in situ* hybridization was done as previously described (Park et al., 2017) using the Affymetrix View RNA ISH kit (Affymetrix, Santa Clara, CA, USA). Briefly, 12 μm tissue sections were fixed at room temperature in 4% paraformaldehyde for 30 min. The tissue sections were treated with protease for 10 min at 40°C. Probes to murine *Meis2* and *Mybl1* (Catalog #VB1-19318, VB1-15979) were hybridized for 3 h at 40°C. Slides were developed for 40 min with the ViewRNA Chromogenic Kit (Fast Red) (Affymetrix) (Park et al., 2017). These slides were then used for a subsequent round of immunostaining as described above.

4.4. RNA and cDNA library prep

E14.5 *C57*BL*/6J* wild-type embryos were collected for culturing as described above. Retinas treated with either 10 μM DAPT or DMSO were grown for 6, 7, 8, 9, 10, 12, 15, 18, 21, 24, or 48 h. Six to eight retinas were pooled for each sample such that all the left eyes and the right eyes of each embryo were included in either the DAPT or the DMSO treatment groups. A single retina from each group was cultured separately and saved for histology (as above, data not shown) to confirm successful DAPT treatment, while the rest were used for RNA isolation. Three replicates for each time-point were collected independently from separate *C57*BL*/6J* litters. The pooled retinas were homogenized in 0.5 mL of TRIzol and the RNA isolated according the manufacturer's protocol (Thermo Fisher Scientific). RNA was further purified using RNeasy kit (Qiagen, Valencia, CA, USA). Samples were then submitted to the University of Colorado Genomics and Microarray Core Facility for quality control, barcoding, and subsequent sequencing (Illumina HiSeq, 2000; Illumina, San Diego, CA, USA).

4.5. RNA sequencing and analysis

Raw reads were processed for Illumina adapters using trimmomatic-0.36 (Bolger et al., 2014). Trimmed sequencing reads were then aligned to the *GRCm38/mm10* version of the reference mouse genome using GSNAP (Wu and Nacu, 2010). Transcripts for uniquely expressed genes were assembled by Cufflinks (Trapnell et al., 2012) and their relative abundances quantified as FPKM (fragments per kilobase exon per million mapped reads) values. PCA analysis of replicate groupings led to an exclusion of individual 12 h, 15 h, and 48 h replicates from the analysis (Fig. S6). Fold change was calculated between treatment groups and differential expression assessed via ANOVA in R to reveal potential candidate genes in the initial screen. Individual genes at each time-point were compared by unpaired t-tests with a false discovery rate (FDR) correction to account for multiple tests. Downstream data filtering and

processing were conducted with Python. To be considered in the top 750 differentially expressed (DE) gene list (Fig. 2B), three criteria had to be met: (1) the mean FPKM had to be higher than 20 in any one sample treatment, (2) the log2 fold change had to be less than -0.5 or greater than 0.5, and (3) the gene had to have a FDR-corrected P-value less than 0.05. Volcano plots were generated using the interactive visualization library Bokeh (Bokeh contributors). Heatmaps were generated using the matrix visualization tool Morpheus (Morpheus).

4.6. Generation of retinal organoids from human iPSCs

Undifferentiated induced pluripotent stem cells (iPSCs) (NCL1, NXCell Inc., Novato, CA) were maintained in Essential 8 Flex medium (Gibco, Grand Island, NY, USA). For generating embryoid bodies (EBs), the cells were dissociated using 0.5 mM EDTA (Corning) in DPBS (Corning) for 4–5 min. The dissociation media was removed and 1.5 mL of ES8 Flex containing 10 μM Y-27632 (Tocris, Minneapolis, MN, USA), was added to each well of a 6-well plate. Cells were gently scraped and transferred to a 15mL tube. The cells were resuspended at a concentration of 4-6 million cells/mL and 60 μL of the suspension was seeded into low attachment microwells (Microtissues Inc., Providence, RI, USA). This yielded about 6,000–9,000 cells per EB. Additional ES8 Flex media with 10 μM Y-27632 was added around the microwells after 30 min. After 24 h, most of the media was removed and changed to media containing DMEM (Gibco), L-ascorbic acid (Sigma, St. Louis, MO, USA), sodium pyruvate, NEAA (Corning), N1 supplement (Sigma), and B27 supplement (Gibco) along with 1% Matrigel (Corning) and 3 μM of IWR-1 (Tocris, Minneapolis, MN, USA). The media was changed daily. IWR-1 was removed on day (D) 7 and Matrigel was removed on D8. Starting around D8, organoids were gently transferred to a suspension plate. On D10, 100 nM SAG (Sigma) was added to the media. From D12 onwards, the cells were maintained in media containing DMEM/F12, 0.5% FBS, NEAA, Sodium Pyruvate, B27 supplement and taurine at 1 μM. 100 nM SAG was added from day 12-19 and 500 nM all-trans retinoic acid (Sigma) was added from D20-75.

4.7. Notch inhibition of human retinal organoids

Six week-differentiated retinal organoids, 5 or 6 per condition, were treated with either 10–25 μM DAPT (data not shown) or 10 μM PF-4014 (PF-03084014 hydrobromide, Sigma) for 3 days and compared to control treated organoids following culture for 11 more days. DAPT-treated organoids had variable outcomes, leading us to utilize PF-4014 treatment for subsequent experiments. Organoids were fixed with cold 4% PFA for 30 min followed by washing with PBS. Tissue was cryopreserved, frozen in OCT, and cryosectioned at 10 μm for histological analysis.

4.8. Retinal organoid immunohistochemistry

Tissue sections were blocked in solution containing PBS with 0.1% Triton X100 and 1% donkey serum for 30 min. Sections were incubated with the primary antibodies overnight at 4°C followed by 3 washes with PBS. The sections were then incubated with fluorescently tagged secondary antibodies (Alexa Fluor 488, 555, 647, Invitrogen, Waltham, MA, USA) for 1 h in the dark at room temperature. Following PBS washes, the sections were incubated in DAPI for 1 min to mark nuclei and mounted with Fluoromount-G. Images were taken with Zeiss LSM510 or LSM700 confocal microscope. Primary antibodies used in this part of the analysis not mentioned previously: rabbit anti-CRX (1:200) (Abcam, Cambridge, UK), goat anti-LHX2 (1:100) (sc-19344, Santa Cruz), rabbit anti-Ki67 (1:250) (AB15580, Abcam), mouse anti-VSX2 (1:100) (Clone:D-11, sc-374151, Santa Cruz), mouse anti-Brn3a (1:100) (sc-8429, Santa Cruz) and rabbit anti-RCVRN (1:100) (AB5585, Millipore). TUNEL was performed using the In Situ Cell Death Detection Kit (Sigma) as per manufacturer guidelines.

Acknowledgements

The authors thank Tania Eliseeva, Grace Randazzo, Tom Reh, Branden Nelson, Byron Hartman, and the CU Denver Genomics and Microarray Core for helpful discussions and technical assistance. The authors thank Jane Johnson for sharing reagents. Work was supported in part by funding from the DOD (W81XWH-14-1-0566) to JAB & DAL and the NIH through grants R01-EY024272 to JAB, R01-EY025779 to DAL, and T32-NS099042 to NBG. Work was partially supported by a Challenge Grant to the CU Department of Ophthalmology from Research to Prevent Blindness, Inc. These experiments were also supported by the Boettcher Foundation and the Lyda Hill Foundation (JAB). Additional support was provided by a core grant from the National Institutes of Health (EY02162) and by Research to Prevent Blindness unrestricted grants to the UCSF Department of Ophthalmology (for DAL).

Appendix A. Supplementary data

Supplementary data to this article can be found online at https://doi.org/10.1016/j.ydbio.2019.05.016.

References

Akimoto, M., Cheng, H., Zhu, D., Brzezinski, J.A., Khanna, R., Filippova, E., Oh, E.C.T., Jing, Y., Linares, J.-L., Brooks, M., Zareparsi, S., Mears, A.J., Hero, A., Glaser, T., Swaroop, A., 2006. Targeting of GFP to newborn rods by Nrl promoter and temporal expression profiling of flow-sorted photoreceptors. Proc. Natl. Acad. Sci. U.S.A. 103, 3890–3895.

Alexiades, M.R., Cepko, C., 1996. Quantitative analysis of proliferation and cell cycle length during development of the rat retina. Dev. Dynam. 205, 293–307.

Applebury, M.L., Farhangfar, F., Glosmann, M., Hashiomoto, K., Kage, K., Robbins, J.T., Shibusawa, N., Wondisford, F.E., Zhang, H., 2007. Transient expression of thyroid hormone nuclear receptor TRbeta2 sets S opsin patterning during cone photoreceptor genesis. Dev. Dynam. 236, 1203–1212.

Baird, N.L., Bowlin, J.L., Cohrs, R.J., Gilden, D., Jones, K.L., 2014. Comparison of varicella-zoster virus RNA sequences in human neurons and fibroblasts. J. Virol. 88, 5877–5880.

Bassett, E.A., Pontoriero, G.F., Feng, W., 2007. Conditional deletion of activating protein 2α (AP-2α) in the developing retina demonstrates non-cell-autonomous roles for AP-2α in optic cup development. Mol. Cell. Biol. 27, 7497–7510.

Bassett, E.A., Korol, A., Deschamps, P.A., Buettner, R., Wallace, V.A., Williams, T., West-Mays, J.A., 2012. Overlapping expression patterns and redundant roles for AP-2 transcription factors in the developing mammalian retina. Dev. Dynam. 241, 814–829.

Bertrand, N., Castro, D.S., Guillemot, F., 2002. Proneural genes and the specification of neural cell types. Nat. Rev. Neurosci. 3, 517–530.

Blackshaw, S., Fraioli, R.E., Furukawa, T., Cepko, C.L., 2001. Comprehensive analysis of photoreceptor gene expression and the identification of candidate retinal disease genes. Cell 107, 579–589.

Bokeh contributors, n.d. Welcome to Bokeh — Bokeh 0.13.0 Documentation [WWW Document]. URL https://bokeh.pydata.org/en/latest/(accessed 9.20.18).

Bolcun-Filas, E., Bannister, L.A., Barash, A., Schimenti, K.J., Hartford, S.A., Eppig, J.J., Handel, M.A., Shen, L., Schimenti, J.C., 2011. A-MYB (MYBL1) transcription factor is a master regulator of male meiosis. Development 138, 3319–3330.

Bolger, A.M., Lohse, M., Usadel, B., 2014. Trimmomatic: a flexible trimmer for Illumina sequence data. Bioinformatics 30, 2114–2120.

Bradford, A.P., Jones, K., Kechris, K., Chosich, J., Montague, M., Warren, W.C., May, M.C., Al-Safi, Z., Kuokkanen, S., Appt, S.E., Polotsky, A.J., 2015. Joint MiRNA/mRNA expression profiling reveals changes consistent with development of dysfunctional corpus luteum after weight gain. PLoS One 10, e0135163.

Brown, N.L., Patel, S., Brzezinski, J., Glaser, T., 2001. Math5 is required for retinal ganglion cell and optic nerve formation. Development 128, 2497–2508.

Brzezinski, J.A., Kim, E.J., Johnson, J.E., Reh, T.A., 2011. Ascl1 expression defines a subpopulation of lineage-restricted progenitors in the mammalian retina. Development 138, 3519–3531.

Brzezinski, J.A., Lamba, D.A., Reh, T.A., 2010. Blimp1 controls photoreceptor versus bipolar cell fate choice during retinal development. Development 137, 619–629.

Brzezinski, J.A., Prasov, L., Glaser, T., 2012. Math5 defines the ganglion cell competence state in a subpopulation of retinal progenitor cells exiting the cell cycle. Dev. Biol. 365, 395–413.

Brzezinski, J.A., Uoon Park, K., Reh, T.A., 2013. Blimp1 (Prdm1) prevents re-specification of photoreceptors into retinal bipolar cells by restricting competence. Dev. Biol. 384, 194–204.

Brzezinski, J.A., Reh, T.A., 2015. Photoreceptor cell fate specification in vertebrates. Development 142, 3263–3273.

Carter-Dawson, L.D., LaVail, M.M., 1979. Rods and cones in the mouse retina. II. Autoradiographic analysis of cell generation using tritiated thymidine. J. Comp. Neurol. 188, 263–272.

Cau, E., Ronsin, B., Bessière, L., Blader, P., 2019. A Notch-mediated, temporal asymmetry in BMP pathway activation promotes photoreceptor subtype diversification. PLoS Biol. 17, e2006250.
Cepko, C., 2014. Intrinsically different retinal progenitor cells produce specific types of progeny. Nat. Rev. Neurosci. 15, 615–627.
Chang, D.H., Cattoretti, G., Calame, K.L., 2002. The dynamic expression pattern of B lymphocyte induced maturation protein-1 (Blimp-1) during mouse embryonic development. Mech. Dev. 117, 305–309.
Chen, S., Wang, Q.L., Nie, Z., Sun, H., Lennon, G., Copeland, N.G., Gilbert, D.J., Jenkins, N.A., Zack, D.J., 1997. Crx, a novel Otx-like paired-homeodomain protein, binds to and transactivates photoreceptor cell-specific genes. Neuron 19, 1017–1030.
Chen, X., Higgins, J., Cheung, S.-T., Li, R., Mason, V., Montgomery, K., Fan, S.-T., van de Rijn, M., So, S., 2004. Novel endothelial cell markers in hepatocellular carcinoma. Mod. Pathol. 17, 1198–1210.
Cherry, T.J., Trimarchi, J.M., Stadler, M.B., Cepko, C.L., 2009. Development and diversification of retinal amacrine interneurons at single cell resolution. Proc. Natl. Acad. Sci. U.S.A. 106, 9495–9500.
Corbo, J.C., Myers, C.A., Lawrence, K.A., Jadhav, A.P., Cepko, C.L., 2007. A typology of photoreceptor gene expression patterns in the mouse. Proc. Natl. Acad. Sci. U.S.A. 104, 12069–12074.
De Melo, J., Qiu, X., Du, G., Cristante, L., Eisenstat, D.D., 2003. Dlx1, Dlx2, Pax6, Brn3b, and Chx10 homeobox gene expression defines the retinal ganglion and inner nuclear layers of the developing and adult mouse retina. J. Comp. Neurol. 461, 187–204.
Doyonnas, R., Nielsen, J.S., Chelliah, S., Drew, E., Hara, T., Miyajima, A., McNagny, K.M., 2005. Podocalyxin is a CD34-related marker of murine hematopoietic stem cells and embryonic erythroid cells. Blood 105, 4170–4178.
Eiraku, M., Takata, N., Ishibashi, H., Kawada, M., Sakakura, E., Okuda, S., Sekiguchi, K., Adachi, T., Sasai, Y., 2011. Self-organizing optic-cup morphogenesis in three-dimensional culture. Nature 472, 51–56.
Eldred, K.C., Hadyniak, S.E., Hussey, K.A., Brenerman, B., Zhang, P., Chamling, X., Sluch, V.M., Welsbie, D.S., Hattar, S., Taylor, J., Wahlin, K., Zack, D.J., Johnston, R.J., 2018. Thyroid hormone signaling specifies cone subtypes in human retinal organoids. Science 362 pii: eaau6348.
Emerson, M.M., Surzenko, N., Goetz, J.J., Trimarchi, J., Cepko, C.L., 2013. Otx2 and Onecut1 promote the fates of cone photoreceptors and horizontal cells and repress rod photoreceptors. Dev. Cell 26, 59–72.
Fossat, N., Le Greneur, C., Béby, F., Vincent, S., Godement, P., Chatelain, G., Lamonerie, T., 2007. A new GFP-tagged line reveals unexpected Otx2 protein localization in retinal photoreceptors. BMC Dev. Biol. 7, 122.
Freund, C.L., Gregory-Evans, C.Y., Furukawa, T., Papaioannou, M., Looser, J., Ploder, L., Bellingham, J., Ng, D., Herbrick, J.A., Duncan, A., Scherer, S.W., Tsui, L.C., Loutradis-Anagnostou, A., Jacobson, S.G., Cepko, C.L., Bhattacharya, S.S., McInnes, R.R., 1997. Cone-rod dystrophy due to mutations in a novel photoreceptor-specific homeobox gene (CRX) essential for maintenance of the photoreceptor. Cell 91, 543–553.
Furukawa, T., Morrow, E.M., Cepko, C.L., 1997. Crx, a novel otx-like homeobox gene, shows photoreceptor-specific expression and regulates photoreceptor differentiation. Cell 91, 531–541.
Furukawa, T., Morrow, E.M., Li, T., Davis, F.C., Cepko, C.L., 1999. Retinopathy and attenuated circadian entrainment in Crx-deficient mice. Nat. Genet. 23, 466–470.
Geling, A., Steiner, H., Willem, M., Bally-Cuif, L., 2002. A γ-secretase inhibitor blocks Notch signaling in vivo and causes a severe neurogenic phenotype in zebrafish. EMBO Rep. 3, 688–694.
Gomes, F.L.A.F., Zhang, G., Carbonell, F., Correa, J.A., Harris, W.A., Simons, B.D., Cayouette, M., 2011. Reconstruction of rat retinal progenitor cell lineages in vitro reveals a surprising degree of stochasticity in cell fate decisions. Development 138, 227–235.
Gonzalez-Cordero, A., Kruczek, K., Naeem, A., Fernando, M., Kloc, M., Ribeiro, J., Goh, D., Duran, Y., Blackford, S.J.I., Abelleira-Hervas, L., Sampson, R.D., Shum, I.O., Branch, M.J., Gardner, P.J., Sowden, J.C., Bainbridge, J.W.B., Smith, A.J., West, E.L., Pearson, R.A., Ali, R.R., 2017. Recapitulation of human retinal development from human pluripotent stem cells generates transplantable populations of cone photoreceptors. Stem Cell Reports 9, 820–837.
Hafler, B.P., Surzenko, N., Beier, K.T., Punzo, C., Trimarchi, J.M., Kong, J.H., Cepko, C.L., 2012. Transcription factor Olig2 defines subpopulations of retinal progenitor cells biased toward specific cell fates. Proc. Natl. Acad. Sci. U.S.A. 109, 7882–7887.
Hendrickson, A.E., Yuodelis, C., 1984. The morphological development of the human fovea. Ophthalmology 91, 603–612.
Hendrickson, A., Possin, D., Vajzovic, L., Toth, C.A., 2012. Histologic development of the human fovea from midgestation to maturity. Am. J. Ophthalmol. 154, 767–778.e2.
Hennig, A.K., Peng, G.-H., Chen, S., 2008. Regulation of photoreceptor gene expression by Crx-associated transcription factor network. Brain Res. 1192, 114–133.
Hlawatsch, J., Karlstetter, M., Aslanidis, A., Lückoff, A., Walczak, Y., Plank, M., Böck, J., Langmann, T., 2013. Sterile alpha motif containing 7 (samd7) is a novel crx-regulated transcriptional repressor in the retina. PLoS One 8, e60633.
Hoshino, A., Ratnapriya, R., Brooks, M.J., Chaitankar, V., Wilken, M.S., Zhang, C., Starostik, M.R., Gieser, L., La Torre, A., Nishio, M., Bates, O., Walton, A., Bermingham-McDonogh, O., Glass, I.A., Wong, R.O.L., Swaroop, A., Reh, T.A., 2017. Molecular anatomy of the developing human retina. Dev. Cell 43, 763–779.e4.
Hsiau, T.H.-C., Diaconu, C., Myers, C.A., Lee, J., Cepko, C.L., Corbo, J.C., 2007. The cis-regulatory logic of the mammalian photoreceptor transcriptional network. PLoS One 2, e643.
Hufnagel, R.B., Le, T.T., Riesenberg, A.L., Brown, N.L., 2010. Neurog2 controls the leading edge of neurogenesis in the mammalian retina. Dev. Biol. 340, 490–503.
Hughes, A.E.O., Enright, J.M., Myers, C.A., Shen, S.Q., Corbo, J.C., 2017. Cell type-specific epigenomic analysis reveals a uniquely closed chromatin architecture in mouse rod photoreceptors. Sci. Rep. 7, 43184.
Inoue, T., Hojo, M., Bessho, Y., Tano, Y., Lee, J.E., Kageyama, R., 2002. Math3 and NeuroD regulate amacrine cell fate specification in the retina. Development 129, 831–842.
Jadhav, A.P., Mason, H.A., Cepko, C.L., 2006. Notch 1 inhibits photoreceptor production in the developing mammalian retina. Development 133, 913–923.
Jasoni, C.L., Reh, T.A., 1996. Temporal and spatial pattern of MASH-1 expression in the developing rat retina demonstrates progenitor cell heterogeneity. J. Comp. Neurol. 369, 319–327.
Jeon, C.J., Strettoi, E., Masland, R.H., 1998. The major cell populations of the mouse retina. J. Neurosci. 18, 8936–8946.
Jiang, Y., Ding, Q., Xie, X., Libby, R.T., Lefebvre, V., Gan, L., 2013. Transcription factors SOX4 and SOX11 function redundantly to regulate the development of mouse retinal ganglion cells. J. Biol. Chem. 288, 18429–18438.
Kang, H.G., Lee, M., Lee, K.B., Hughes, M., Kwon, B.S., Lee, S., McNagny, K.M., Ahn, Y.H., Ko, J.M., Ha, I.-S., Choi, M., Cheong, H.I., 2017. Loss of podocalyxin causes a novel syndromic type of congenital nephrotic syndrome. Exp. Mol. Med. 49, e414.
Katoh, K., Omori, Y., Onishi, A., Sato, S., Kondo, M., Furukawa, T., 2010. Blimp1 suppresses Chx10 expression in differentiating retinal photoreceptor precursors to ensure proper photoreceptor development. J. Neurosci. 30, 6515–6526.
Kay, J.N., Finger-Baier, K.C., Roeser, T., Staub, W., Baier, H., 2001. Retinal ganglion cell genesis requires lakritz, a Zebrafish atonal Homolog. Neuron 30, 725–736.
Kerjaschki, D., Sharkey, D.J., Farquhar, M.G., 1984. Identification and characterization of podocalyxin–the major sialoprotein of the renal glomerular epithelial cell. J. Cell Biol. 98, 1591–1596.
Koike, C., Nishida, A., Ueno, S., Saito, H., Sanuki, R., Sato, S., Furukawa, A., Aizawa, S., Matsuo, I., Suzuki, N., Kondo, M., Furukawa, T., 2007. Functional roles of Otx2 transcription factor in postnatal mouse retinal development. Mol. Cell. Biol. 27, 8318–8329.
Kowalchuk, A.M., Maurer, K.A., Shoja-Taheri, F., Brown, N.L., 2018. Requirements for Neurogenin2 during mouse postnatal retinal neurogenesis. Dev. Biol. 442, 220–235.
Kuribayashi, H., Baba, Y., Watanabe, S., 2014. BMP signaling participates in late phase differentiation of the retina, partly via upregulation of Hey2. Dev Neurobiol 74, 1172–1183.
Kühn, H., 1978. Light-regulated binding of rhodopsin kinase and other proteins to cattle photoreceptor membranes. Biochemistry 17, 4389–4395.
Lakowski, J., Han, Y.-T., Pearson, R.A., Gonzalez-Cordero, A., West, E.L., Gualdoni, S., Barber, A.C., Hubank, M., Ali, R.R., Sowden, J.C., 2011. Effective transplantation of photoreceptor precursor cells selected via cell surface antigen expression. Stem Cell. 29, 1391–1404.
la Vail, M.M., Rapaport, D.H., Rakic, P., 1991. Cytogenesis in the monkey retina. J. Comp. Neurol. 309, 86–114.
Liu, W., Wang, J.-H., Xiang, M., 2000. Specific expression of the LIM/homeodomain protein Lim-1 in horizontal cells during retinogenesis. Dev. Dynam. 217, 320–325.
Marquardt, T., Ashery-Padan, R., Andrejewski, N., Scardigli, R., Guillemot, F., Gruss, P., 2001. Pax6 is required for the multipotent state of retinal progenitor cells. Cell 105, 43–55.
Mears, A.J., Kondo, M., Swain, P.K., Takada, Y., Bush, R.A., Saunders, T.L., Sieving, P.A., Swaroop, A., 2001. Nrl is required for rod photoreceptor development. Nat. Genet. 29, 447–452.
Meyer-Franke, A., Kaplan, M.R., Pfrieger, F.W., Barres, B.A., 1995. Characterization of the signaling interactions that promote the survival and growth of developing retinal ganglion cells in culture. Neuron 15, 805–819.
Mills, T.S., Eliseeva, T., Bersie, S.M., Randazzo, G., Nahreini, J., Park, K.U., Brzezinski, J.A., 4th, 2017. Combinatorial regulation of a Blimp1 (Prdm1) enhancer in the mouse retina. PLoS One 12, e0176905.
Mizeracka, K., Trimarchi, J.M., Stadler, M.B., Cepko, C.L., 2013. Analysis of gene expression in wild-type and Notch1 mutant retinal cells by single cell profiling. Dev. Dynam. 242, 1147–1159.
Moore, K.B., Logan, M.A., Aldiri, I., Roberts, J.M., Steele, M., Vetter, M.L., 2018. C8orf46 homolog encodes a novel protein Vexin that is required for neurogenesis in Xenopus laevis. Dev. Biol. 437, 27–40.
Morpheus [WWW Document], n.d. URL https://software.broadinstitute.org/morpheus/ (accessed 9.20.18).
Muranishi, Y., Terada, K., Inoue, T., Katoh, K., 2011. An essential role for RAX homeoprotein and NOTCH–HES signaling in Otx2 expression in embryonic retinal photoreceptor cell fate determination. J. Neurosci. 31, 16792–16807.
Nakano, T., Ando, S., Takata, N., Kawada, M., Muguruma, K., Sekiguchi, K., Saito, K., Yonemura, S., Eiraku, M., Sasai, Y., 2012. Self-formation of optic cups and storable stratified neural retina from human ESCs. Cell Stem Cell 10, 771–785.
Nelson, B.R., Hartman, B.H., Georgi, S.A., Lan, M.S., Reh, T.A., 2007. Transient inactivation of Notch signaling synchronizes differentiation of neural progenitor cells. Dev. Biol. 304, 479–498.
Ney, J.T., Zhou, H., Sipos, B., Büttner, R., Chen, X., Klöppel, G., Gütgemann, I., 2007. Podocalyxin-like protein 1 expression is useful to differentiate pancreatic ductal adenocarcinomas from adenocarcinomas of the biliary and gastrointestinal tracts. Hum. Pathol. 38, 359–364.
Ng, L., Hurley, J.B., Dierks, B., Srinivas, M., Saltó, C., Vennström, B., Reh, T.A., Forrest, D., 2001. A thyroid hormone receptor that is required for the development of green cone photoreceptors. Nat. Genet. 27, 94–98.
Nishida, A., Furukawa, A., Koike, C., Tano, Y., Aizawa, S., Matsuo, I., Furukawa, T., 2003. Otx2 homeobox gene controls retinal photoreceptor cell fate and pineal gland development. Nat. Neurosci. 6, 1255–1263.
Olsauskas-Kuprys, R., Zlobin, A., Osipo, C., 2013. Gamma secretase inhibitors of Notch signaling. OncoTargets Ther. 6, 943–955.
Omori, Y., Kubo, S., Kon, T., Furuhashi, M., Narita, H., Kominami, T., Ueno, A., Tsutsumi, R., Chaya, T., Yamamoto, H., Suetake, I., Ueno, S., Koseki, H.,

Nakagawa, A., Furukawa, T., 2017. Samd7 is a cell type-specific PRC1 component essential for establishing retinal rod photoreceptor identity. Proc. Natl. Acad. Sci. U.S.A. 114, E8264–E8273.
Panza, F., Frisardi, V., Imbimbo, B.P., 2010. γ-Secretase inhibitors for the treatment of Alzheimer's disease: the current state. CNS Neurosci. Ther. 16, 272–284.
Park, K.U., Randazzo, G., Jones, K.L., Brzezinski, J.A., 4th, 2017. Gsg1, Trnp1, and Tmem215 mark subpopulations of bipolar interneurons in the mouse retina. Investig. Ophthalmol. Vis. Sci. 58, 1137–1150.
Peng, Y.-R., Shekhar, K., Yan, W., Herrmann, D., Sappington, A., Bryman, G.S., van Zyl, T., Do, M.T.H., Regev, A., Sanes, J.R., 2019. Molecular classification and comparative taxonomics of foveal and peripheral cells in primate retina. Cell 176, 1222–1237.
Perron, M., Harris, W.A., 2000. Determination of vertebrate retinal progenitor cell fate by the Notch pathway and basic helix-loop-helix transcription factors. Cell. Mol. Life Sci. 57, 215–223.
Pollak, J., Wilken, M.S., Ueki, Y., Cox, K.E., Sullivan, J.M., Taylor, R.J., Levine, E.M., Reh, T.A., 2013. ASCL1 reprograms mouse Müller glia into neurogenic retinal progenitors. Development 140, 2619–2631.
Rapaport, D.H., Vietri, A.J., 1991. Identity of cells produced by two stages of cytogenesis in the postnatal cat retina. J. Comp. Neurol. 312, 341–352.
Rapaport, D.H., Wong, L.L., Wood, E.D., Yasumura, D., LaVail, M.M., 2004. Timing and topography of cell genesis in the rat retina. J. Comp. Neurol. 474, 304–324.
Riesenberg, A.N., Liu, Z., Kopan, R., Brown, N.L., 2009. Rbpj cell autonomous regulation of retinal ganglion cell and cone photoreceptor fates in the mouse retina. J. Neurosci. 29, 12865–12877.
Roberts, M.R., Hendrickson, A., McGuire, C.R., Reh, T.A., 2005. Retinoid X receptor γ is necessary to establish the S-opsin gradient in cone photoreceptors of the developing mouse retina. Investig. Ophthalmol. Vis. Sci. 46, 2897–2904.
Roberts, M.R., Srinivas, M., Forrest, D., Morreale de Escobar, G., Reh, T.A., 2006. Making the gradient: thyroid hormone regulates cone opsin expression in the developing mouse retina. Proc. Natl. Acad. Sci. U.S.A. 103, 6218–6223.
Sapkota, D., Chintala, H., Wu, F., Fliesler, S.J., Hu, Z., Mu, X., 2014. Onecut1 and Onecut2 redundantly regulate early retinal cell fates during development. Proc. Natl. Acad. Sci. U.S.A. 111, E4086–E4095.
Sassetti, C., Tangemann, K., Singer, M.S., Kershaw, D.B., Rosen, S.D., 1998. Identification of podocalyxin-like protein as a high endothelial venule ligand for L-selectin: parallels to CD34. J. Exp. Med. 187, 1965–1975.
Sato, S., Inoue, T., Terada, K., Matsuo, I., Aizawa, S., Tano, Y., Fujikado, T., Furukawa, T., 2007. Dkk3-Cre BAC transgenic mouse line: a tool for highly efficient gene deletion in retinal progenitor cells. Genesis 45, 502–507.
Schneider, C.A., Rasband, W.S., Eliceiri, K.W., 2012. NIH Image to ImageJ: 25 years of image analysis. Nat. Methods 9, 671–675.
Siemerink, M.J., Hughes, M.R., Dallinga, M.G., Gora, T., Cait, J., Vogels, I.M.C., Yetin-Arik, B., Van Noorden, C.J.F., Klaassen, I., McNagny, K.M., Schlingemann, R.O., 2016. CD34 promotes pathological epi-retinal neovascularization in a mouse model of oxygen-induced retinopathy. PLoS One 11, e0157902.
Sloan, K.R., Kalina, R.E., Hendrickson, A.E., 1990. Human photoreceptor topography. J. Comp. Neurol. 292, 497–523.
Smiley, S., Nickerson, P.E., Comanita, L., Daftarian, N., El-Sehemy, A., Tsai, E.L.S., Matan-Lithwick, S., Yan, K., Thurig, S., Touahri, Y., Dixit, R., Aavani, T., De Repentingy, Y., Baker, A., Tsilfidis, C., Biernaskie, J., Sauvé, Y., Schuurmans, C., Kothary, R., Mears, A.J., Wallace, V.A., 2016. Establishment of a cone photoreceptor transplantation platform based on a novel cone-GFP reporter mouse line. Sci. Rep. 6, 22867.
Surzenko, N., Crowl, T., Bachleda, A., Langer, L., 2013. SOX2 maintains the quiescent progenitor cell state of postnatal retinal Müller glia. Development 140, 1445–1456.
Taranova, O.V., Magness, S.T., Fagan, B.M., Wu, Y., Surzenko, N., Hutton, S.R., Pevny, L.H., 2006. SOX2 is a dose-dependent regulator of retinal neural progenitor competence. Genes Dev. 20, 1187–1202.
Tomita, K., Nakanishi, S., Guillemot, F., Kageyama, R., 1996. Mash1 promotes neuronal differentiation in the retina. Genes Cells 1, 765–774.
Trapnell, C., Roberts, A., Goff, L., Pertea, G., Kim, D., Kelley, D.R., Pimentel, H., Salzberg, S.L., Rinn, J.L., Pachter, L., 2012. Differential gene and transcript expression analysis of RNA-seq experiments with TopHat and Cufflinks. Nat. Protoc. 7, 562–578.
Vitureira, N., Andrés, R., Pérez-Martínez, E., Martínez, A., Bribián, A., Blasi, J., Chelliah, S., López-Doménech, G., De Castro, F., Burgaya, F., McNagny, K., Soriano, E., 2010. Podocalyxin is a novel polysialylated neural adhesion protein with multiple roles in neural development and synapse formation. PLoS One 5, e12003.
Vitureira, N., McNagny, K., Soriano, E., Burgaya, F., 2005. Pattern of expression of the podocalyxin gene in the mouse brain during development. Gene Expr. Patterns 5, 349–354.
Völkner, M., Zschätzsch, M., Rostovskaya, M., Overall, R.W., Busskamp, V., Anastassiadis, K., Karl, M.O., 2016. Retinal organoids from pluripotent stem cells efficiently recapitulate retinogenesis. Stem Cell Reports 6, 525–538.
Wall, D.S., Mears, A.J., McNeill, B., Mazerolle, C., Thurig, S., Wang, Y., Kageyama, R., Wallace, V.A., 2009. Progenitor cell proliferation in the retina is dependent on Notch-independent Sonic hedgehog/Hes1 activity. J. Cell Biol. 184, 101–112.
Walther, C., Gruss, P., 1991. Pax-6, a murine paired box gene, is expressed in the developing CNS. Development 113, 1435–1449.
Wang, S., Sengel, C., Emerson, M.M., Cepko, C.L., 2014. A gene regulatory network controls the binary fate decision of rod and bipolar cells in the vertebrate retina. Dev. Cell 30, 513–527.
Wang, S.W., Kim, B.S., Ding, K., Wang, H., Sun, D., Johnson, R.L., Klein, W.H., Gan, L., 2001. Requirement for math5 in the development of retinal ganglion cells. Genes Dev. 15, 24–29.
Wei, P., Walls, M., Qiu, M., Ding, R., Denlinger, R.H., Wong, A., Tsaparikos, K., Jani, J.P., Hosea, N., Sands, M., Randolph, S., Smeal, T., 2010. Evaluation of selective gamma-secretase inhibitor PF-03084014 for its antitumor efficacy and gastrointestinal safety to guide optimal clinical trial design. Mol. Cancer Ther. 9, 1618–1628.
Welby, E., Lakowski, J., Di Foggia, V., Budinger, D., Gonzalez-Cordero, A., Lun, A.T.L., Epstein, M., Patel, A., Cuevas, E., Kruczek, K., Naeem, A., Minneci, F., Hubank, M., Jones, D.T., Marioni, J.C., Ali, R.R., Sowden, J.C., 2017. Isolation and comparative transcriptome analysis of human fetal and ipsc-derived cone photoreceptor cells. Stem Cell Reports 9, 1898–1915.
Wilden, U., Hall, S.W., Kühn, H., 1986. Phosphodiesterase activation by photoexcited rhodopsin is quenched when rhodopsin is phosphorylated and binds the intrinsic 48-kDa protein of rod outer segments. Proc. Natl. Acad. Sci. U.S.A. 83, 1174–1178.
Wong, L.L., Rapaport, D.H., 2009. Defining retinal progenitor cell competence in Xenopus laevis by clonal analysis. Development 136, 1707–1715.
Wu, F., Li, R., Umino, Y., Kaczynski, T.J., Sapkota, D., Li, S., Xiang, M., Fliesler, S.J., Sherry, D.M., Gannon, M., Solessio, E., Mu, X., 2013. Onecut1 is essential for horizontal cell genesis and retinal integrity. J. Neurosci. 33, 13053–13065, 13065a.
Wu, F., Sapkota, D., Li, R., Mu, X., 2012. Onecut 1 and Onecut 2 are potential regulators of mouse retinal development. J. Comp. Neurol. 520, 952–969.
Wu, T.D., Nacu, S., 2010. Fast and SNP-tolerant detection of complex variants and splicing in short reads. Bioinformatics 26, 873–881.
Xiang, M., Zhou, L., Macke, J.P., Yoshioka, T., Hendry, S.H., Eddy, R.L., Shows, T.B., Nathans, J., 1995. The Brn-3 family of POU-domain factors: primary structure, binding specificity, and expression in subsets of retinal ganglion cells and somatosensory neurons. J. Neurosci. 15, 4762–4785.
Yang, Z., Ding, K., Pan, L., Deng, M., Gan, L., 2003. Math5 determines the competence state of retinal ganglion cell progenitors. Dev. Biol. 264, 240–254.
Yaron, O., Farhy, C., Marquardt, T., Applebury, M., Ashery-Padan, R., 2006. Notch1 functions to suppress cone-photoreceptor fate specification in the developing mouse retina. Development 133, 1367–1378.
Young, R.W., 1985. Cell differentiation in the retina of the mouse. Anat. Rec. 212, 199–205.
Zhang, J., Zhu, Z., Wu, H., Yu, Z., Rong, Z., Luo, Z., Xu, Y., Huang, K., Qiu, Z., Huang, C., 2019. PODXL, negatively regulated by KLF4, promotes the EMT and metastasis and serves as a novel prognostic indicator of gastric cancer. Gastric Cancer 22, 48–59.
Zhu, J., Reynolds, J., Garcia, T., Cifuentes, H., Chew, S., Zeng, X., Lamba, D.A., 2018. Generation of transplantable retinal photoreceptors from a current good manufacturing practice-manufactured human induced pluripotent stem cell line. Stem Cells Transl. Med. 7, 210–219.